Detection of fouling in heat exchangers

An dissertation by
Oddgeir Guðmundsson

submitted to the Faculty of Engineering in partial fulfillment of the requirements for the degree of M.Sc.

University of Iceland 2008
HI-MS-2008

University of Iceland
Faculty of Engineering
VR-II, Hjarðarhaga 2-6, IS-107 Reykjavik, Iceland
Phone +354 525 4648, Fax +354 525 4632
verk@hi.is
www.hi.is

Abstract

The aim of this study is to investigate the possibility of using statistical methods, for example state space models and Kalman filters, to detect fouling in cross-flow heat exchangers. This was done dy using measurements that are taken in normal operation of the heat exchanger. That is the inlet and outlet temperatures and the mass flow for the hot and cold fluid. Models were derived for on-line and off-line detection and the performance of the methods were compared.

It is difficult to get access to data from cross-flow heat exchangers. Therefore a simulated data from cross-flow heat exchanger was used. In the simulation it is possible to keep the heat exchanger clean to a certain point and then introduce fouling.

The off-line and on-line methods are build up by dividing the heat exchanger into sections. The states (temperatures) in the sections are represented with physical equations and the Kalman filter is used to estimate the states. Fouling detection is done by monitoring parameters of the model.

The conclusion is that it is possible to detect fouling in cross-flow heat exchangers with the above mentioned methods. The off-line method detects the fouling faster than the on-line method.

If the variations in the inputs are limited, the use of previous mentioned methods is not possible. Therefore a new method was derived, here called the slope method. By plotting the heat transfer, $\dot{m}c\Delta T$, versus the log mean temperature difference, ΔT_{LMTD}, the slope through the points should be equal to AU. Fouling is detected by monitoring for changes in the slope.

Ágrip

Markmið þessa verkefnis er að rannsaka hvort hægt sé að nota tölfræðilegar aðferðir, svo sem ástandslíkön og Kalman síur, til að greina útfellingar í krossflæðis varmaskiptum, eingöngu með því að nota mælingar sem mældar eru í venjulegri notkun. Fundin voru líkön fyrir rauntíma og ekki-rauntíma greiningu og kannað hver mismunurinn á árangri aðferðanna er.

Erfitt var að nálgast gögn úr krossflæðis varmaskiptum meðan á rannsókn þessari stóð og því var notast við hermd gögn. Í hermuninni er hægt að stjórna hvenær útfellingarnar byrja og hversu miklar þær eru.

Í rauntíma og ekki-rauntíma aðferðunum er varmaskiptinum skipt upp í hólf og eru eðlisfræðilegar jöfnur notaðar til að lýsa ástöndunum í hólfunum. Kalman sía er notuð til að meta ástöndin í hólfunum og stikar undirliggjandi líkans metnir út frá ástöndunum. Við greiningu á útfellingum er fylgst með hliðrunum í stikum líkansins.

Helstu niðurstöður eru að hægt er að greina útfellingar í krossflæðis varmaskiptum með ofan nefndum aðferðum. Ekki-rauntíma aðferðin greinir útfellingar fyrr en rauntíma aðferðin.

Ef takmarkaður breytileiki er í inn- og útmerkjum varmaskiptisins er ekki hægt að nota ofangreindar aðferðir og því var fundin ný aðferð sem er kölluð hallatölu aðferðin. Með því að teikna varmaflutninginn, $\dot{m}c\Delta T$, á móti lógaritmíska meðalhitanum, ΔT_{LMTD}, ætti hallatala línunnar í gegnum punktanna að jafngilda AU. Útfellingar eru greindar með því að fylgjast með breytingum á hallatölunni.

Preface

This M.Sc. project was carried out at the Department of Mechanical and Industrial Engineering at the University of Iceland.

First of all I would like to thank my supervisors, professor Olafur Petur Palsson and assoc. professor Halldor Palsson both at the Department of Mechanical and Industrial Engineering, for their time, co-operation and support throughout this work. I would also like to thank professor Sylvain Lalot at the Univeristé de Valenciennes in France, specially for answering many of my questions and for his hospitality in our visit to France. Furthermore would I like to thank Steinthor Oddgeirson for proof reading. In addition I would like to thank my family, friends and my partner, Sigrun, for their support and encouragement throughout my studies.

During this work the powerplants Svartsengi at Reykjanes and Hellisheidavirkjun were visited. I would like to thank Hitaveita Sudurnesja and Orkuveita Reykjavikur for making those visits possible.

To all others not mentioned: Thanks.

The study was sponsored by the University of Iceland - Research fund and the France-Icelandic Jule Verne fund.

Reykjavik, June 2008.

Oddgeir Gudmundsson.

Contents

Nomenclature

$\dot{m}$	mass flow rate
$\dot{Q}$	heat transfer rate
$\frac{\partial}{\partial v}$	derivative with respect to variable v
$\frac{d}{dt}$	derivative with respect to time
μ	dynamic viscosity
ν	kinematic viscosity
ρ	density
$\underline{\dot{m}}$	mass flow rate state vector
$\underline{f}$	state matrix
$\underline{T}$	temperature state vector
$\underline{u}$	state vector
$\underline{w}$	noise state vector
$\underline{x}$	overall state vector
$\underline{z}$	measurement vector
A	state matrix or surface area for heat transfer
B	state matrix
C	constant
c	constant or specific heat when used with a subscript

Dh hydraulic diameter

F correction factor for temperature difference in cross-flow heat exchangers

F state matrix

H measurement matrix

h threshold coefficient or convection coefficient when used with a subscript

K Kalman gain matrix or constant when used with subscripts c or h

k discrete time index

k thermal conductivity

M mass of fluid in one section

ns number of sections, n sections in x-direction and s sections in y-direction

Nu Nusselt number

P covariance error matrix

Pr Prandt number

Q covariance matrix or heat transfer rate when used with a dot

R measurement noise covariance

R_f fouling factor

R_th thermal resistance of metal between the two fluids

Re Reynolds number

T temperature

t time

U overall heat transfer coefficient

w process noise

w white Gaussian noise sequence with zero mean and covariance matrix Q

y exponent of the Reynolds number in a convection correlation

Greek symbols

α model parameter

β model parameter

Δt time step

Δ difference

ϵ error

τ model parameter

$\underline{\theta}$ parameter state vector

Subscripts

α relative to the model parameter α

β relative to the model parameter β

θ relative to the parameter state vector

c cold sign

f relative to the state space function

h hot side

i in section i

in inlet

k at discrete time index k

$LMTD$ log mean temperature difference

m metal

out outlet

z relative to the measurement

Superscript

$*$ relative to the reference state

$-$ a priori state estimate

$\wedge$ a posteriori state estimate

T transpose

1 Introduction

When using heat exchangers it is always the possibility that fouling will occur. That is the metal that is placed between the cold and hot flow in the heat exchanger a) accumulates deposits from the fluids, b) builds up biofilm and c) starts to rust. It is important to minimize fouling in heat exchangers, especially in district heating systems where heat transfer is large. As the fouling increases the heat transfer coefficient decreases which will increase the energy cost of the heat exchanger. For example, at the Vestegnens Kraftvarmeselskab in Denmark, it is said that for every 5°C temperature increase for which the hot water flowing into the heat exchangers must be heated because of fouling, is an added 800-940 k euro/year cost for the consumer, [11]. In fact total cost of fouling in heat exchangers in highly industrialized countries are approximately 0.25% of gross national production, [24] and [31].

Fouling also has an effect on the environment since the increased resistance from fouling will increase power consumption. For instance in a 550 MW coal-fired power plant a fouling biofilm of 200μm lead to increase of about 12 tons of CO_2 per day, [5].

Due to the cost and the environmental issues introduced with fouling, it is preferred to take steps to detect or reduce fouling if possible. Effective fouling mitigation techniques include, [30].

- Reduce the rate of fouling by adding chemical materials into the flow.
- Increase the heat transfer area of the heat exchanger.
- Clean the heat exchangers when they get fouled.

Research of fouling, both causes and detection, has been studied and still is ex-

tensively studied. Studies of causes of fouling are for example [28] and [24] where modifications of the heat transfer surface is studied and ion implantation of fluorine and silicon ion into the heater alloys are studied respectively . Studies of detection of fouling are for example [10] and [25] where the thermal efficiency and temperature drop in the outlets are studied respectively. Research of fouling in heat exchangers are a challenge and conferences are regularly organized, see for example http://www.engconfingl.org/.

The classical detection methods are, [16]:

1. Examination of the heat transfer coefficient.
2. Simultaneous observations of pressure drops and mass flow rates.
3. Temperature measurements.
4. Ultrasonic or electrical measurements.
5. Weighing of heat exchanger plates.

Methods based on (1-3) require that the system presents successive steady behavior for some period of time. Methods based on (4) only monitor local fouling. Method (5) requires that the process is stopped. The restrictions in (1-4) can be too strict and the requirement of (5) can be too costly to be economical.

Another approach is to model the heat exchanger and look for any discrepancy between model predictions and what is actually measured. The aim of this study is to show how a physical state space model can be used to detect fouling in a cross-flow heat exchanger. The model will be based on the mass flow rates and the inlet/outlet temperatures.

In cases like heat exchangers where it is not possible to observe the model states of interest, the Kalman filter can be used to estimate the unobservable states by using the observable states. That is by using the inputs and outputs of the process. The Kalman filter has been used in many different areas of studies where the state of interest is not observable. As an example, in [12] the Kalman filter was used in flood forecasting for the river Fnjóská in Northern Iceland. In that study the inputs to the model were precipitation, either snow or rain, and the output was the water flow in the river. The states of the models were water that was bound in the snow and the water on the watershed of the river.

Detection of fouling in heat exchangers have been studied extensively and the following list summarizes just few of the methods for fouling detection.

- In [34] a good overview of the use of ultrasonics, acoustic and optical techniques to detect fouling on-line is presented.
- In [18] the heat exchanger is modeled with neural networks and in [17] the neural network is used to detect fouling on-line.
- In [7] a measurements of electric resistance is used to detect fouling build up in the heat exchanger.
- In [16] extended Kalman filter is used to detect fouling in counter-flow heat exchangers.

1.1 Introduction to the thesis

The main references of this study are [17], [16], [14], [15] and [13] where state space methods were used to detect fouling in parallel- and counter-flow heat exchangers.

In the first part, a general discussion about heat exchangers is given. Then the physics behind the study and a brief description of the statistical methods such as the Kalman filters are given. Then the three methods are derived.

1. **Off-line method** where standard Kalman filter is used.
2. **On-line method** where extended Kalman filter is used.
3. **Slope method**.

Following a description of the methods a short discussion about the Cumulative sum control chart, CuSum chart, is given. The CuSum chart is a statistical method to detect changes in time series. After the theory chapter a presentation of the data used in the study is given. In the result chapter the results for each of the methods will be given separately. Following the result chapter a discussion about the methods and their results are given. Following the discussion chapter a conclusion of the study is given.

2 Heat exchangers

Heat exchangers are common devices in many different industrial fields, as in the chemical-, petrochemical-, energy- and food-industry and they are also widely used by the public in air conditioning and house heating. A heat exchanger is a device in which energy is transferred from one fluid to another across a solid surface or by mixing of the fluids. Heat exchanger analysis and design therefore involves both convection, from fluid to solid surface or vice versa, and conduction through the solid surface. There can also be radiative heat transfer inside the heat exchanger. Radiative transfer between the heat exchanger and the environment can usually be neglected unless the heat exchanger is uninsulated and its external surfaces are very hot.

For efficiency, the heat exchangers are designed to maximize the surface area that exists between the fluids and make sure the separating material has as little resistance to heat transfer as possible. Heat exchangers are also designed so that resistance to fluid flows is as small as possible. By inducing turbulent flow in the fluids it is possible to get better efficiency than with laminar flow of the fluids, [6].

When heat exchangers have been in operation for some time fouling starts building up on the separating material between the fluids, which will increase the resistance of heat transfer and decrease the efficiency of the heat exchanger. Because of fouling, it is necessary to clean or replace the heat exchanger regularly.

Selection of heat exchanger for a particular use can be very complicated because of the wide range of available heat exchangers and the many variables involved, [6, 27] and [33]. Few of the important factors that should be addressed before choosing a heat exchanger are.

- Required heat transfer rate.
- Size and weight.
- High/low pressure limits.
- Allowable temperature ranges.
- Pressure drop across the heat exchanger.
- Cleaning ability, maintenance and repair.
- Operational environment.

In a manufacturing industry there are typically many different types of heat exchangers used in the process to the final production. Choosing the wrong heat exchanger in any stage of the process can result in a costly production downtime and high maintenance cost.

2.1 Flow arrangements in heat exchangers

Heat Exchangers are commonly classified according to their flow arrangement.

- Parallel-flow.
- Counter-flow.
- Cross-flow.

The main difference between these classifications is the temperature variation through the heat exchangers. The temperature variations have considerable effect on the heat transfer of the heat exchanger, the higher the temperature difference between the hot and cold side is the higher the heat transfer will be. A common measurements of the temperature difference are the arithmetic mean temperature difference and the log mean temperature difference.

The arithmetic mean temperature difference, ΔT assumes that the temperature drops linearly throughout the heat exchanger. The log mean temperature difference, Δ_{LMTD}, is a logarithmic average of the temperature difference and is an exact representation of the temperature profile of the heat exchanger.

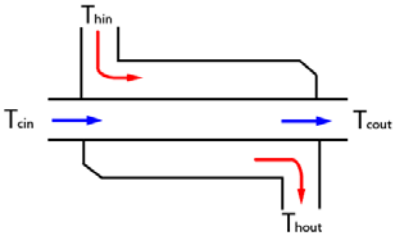

Figure 2.1: Parallel-flow heat exchanger

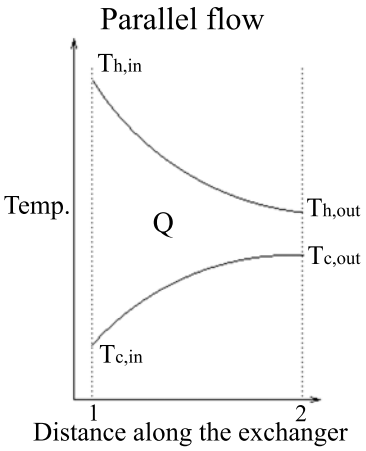

Figure 2.2: The temperature profile for Parallel-flow heat exchanger

2.1.1 Parallel-flow

In this type of heat exchanger the two fluids enter the heat exchanger at the same end and travel in parallel to one another through the heat exchanger to the other side, see Figure 2.1.

In this case, the two fluids enter the heat exchanger from the same end with a large temperature difference. As the heat is transferred from the hot fluid to the cold one, their temperatures difference decreases. Figure 2.2 shows the temperature difference along the heat exchanger. It can clearly be seen that the heat transfer rate is highest at the inlet and then the heat transfer rate gradually diminishes as the fluids travel along the heat exchanger. If the heat exchanger is big the output temperature of the cold flow can be really close to the output temperature of the hot flow.

2.1.2 Counter-flow

Unlike in the parallel-flow heat exchanger the two fluids enter the heat exchanger from opposite ends and travel against one another through the cross-flow heat exchanger, see Figure 2.3.

In this case the cold fluid exits the heat exchanger where the hot fluid enters the heat exchanger and therefore it will approach the inlet temperature of the fluid through the whole heat exchanger, see Figure 2.4.

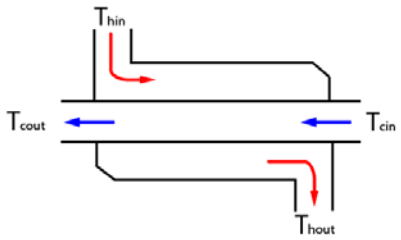

Figure 2.3: Counter-flow heat exchanger

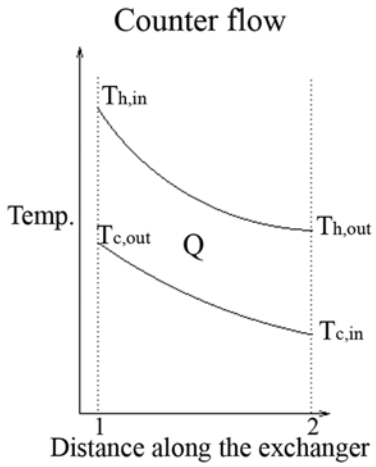

Figure 2.4: The temperature profile for Counter-flow heat exchanger

When comparing Figures 2.2 and 2.4, it can be seen that unlike the parallel-flow heat exchanger, the output of the cold fluid in the counter-flow heat exchanger can become hotter than the output of the hot fluid.

In fact the counter flow heat exchanger is the most efficient of the three types. The efficiency of a counter flow heat exchanger is due to the fact that the average ΔT (dif-

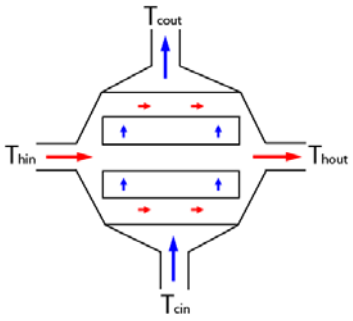

Figure 2.5: Cross-flow heat exchanger

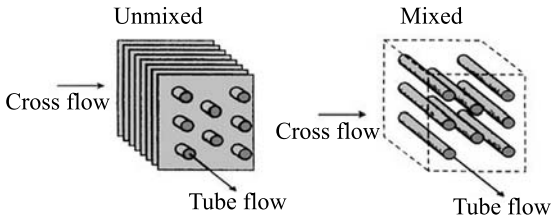

Figure 2.6: Cross-flow heat exchanger, mixed and unmixed flow

ference in temperature) between the two fluids over the length of the heat exchanger can be minimized. This means that the log mean temperature difference (LMTD) for a counter flow heat exchanger is smaller than the LMTD for a similar parallel or cross-flow heat exchanger.

2.1.3 Cross-flow

In a cross-flow heat exchanger the two fluids enter the heat exchanger perpendicular to one another and travel perpendicular to one another through the heat exchanger i.e., one fluid flows through tubes and the second fluid passes around the tubes at 90° angle, see Figure 2.5.

In a cross-flow heat exchanger one of the fluid travels through the heat exchanger in unmixed tubes while the other can travel either mixed or unmixed perpendicular to the other one through the heat exchanger, see Figure 2.6. Mixing the fluids can significantly alter the heat transfer characteristics of the heat exchanger.

Cross-flow heat exchangers are mainly used when the state of one fluid changes as

it travels through the heat exchanger. For instance steam condenser in steam power plants is usually a cross-flow heat exchanger. When the steam comes out of the turbines and enters the heat exchanger the heat will transfer from the steam to the colder fluid, which flows through tubes, and hence condensing the steam to a fluid. Large volumes of vapor may be condensed by using this type of heat exchangers.

Another common use of cross-flow heat exchanger is in automotive radiators. The automotive radiator is a cross-flow water-to-air heat exchanger with both fluids unmixed. The water flows in tubes and the air flows between.

The log mean temperature difference, LMTD, mentioned earlier is for the parallel-flow and counter-flow heat exchangers only. In [6] it is recommended to relate the equivalent temperature difference to the log mean temperature difference relation of the counter-flow case with a correction factor F, where F is equal or less than 1.

In fact the cross-flow heat exchanger is somewhere between the counter-flow and parallel-flow in efficiency.

2.2 Different types of heat exchangers

Another way of classifying heat exchangers than by their flow arrangements, is by their construction, which involve for example, [6, 33] and [1].

- Shell-and-tube heat exchangers.
- Plate heat exchangers.
- Regenerative heat exchangers.
- Adiabatic wheel heat exchangers.
- Fluid heat exchangers.
- Dynamic scraped surface heat exchangers.
- Phase-change heat exchangers.
- HVAC air coils.
- Spiral heat exchangers.

The two most common types of heat exchangers are the shell-and-tube and the plate heat exchangers. A brief discussion about these types of heat exchangers is given in the following chapters.

2.2.1 Shell-and-tube heat exchangers

The shell-and-tube heat exchangers are typically used for high pressure applications and are perhaps the most common types of heat exchangers that are used in industrial applications. Shell-and-tube heat exchangers contain a large number of tubes which can contain fluid that is either intended to cool or heat. The tubes are packed in a shell with their axes parallel to that of the shell. The second fluid runs in the shell over the tubes and it can either provide the heat or absorb the heat from the fluid in the tube. The tubes are usually kept with fixed and equal space between each other with baffles, which also force the shell-side fluid to flow across the shell to enhance heat transfer. If there are four baffles in the heat exchanger it is called either four- or five-shell pass heat exchanger, depending on how many times the shell-fluid travels across the shell. It is also possible to let the tube change direction inside the shell. If the tube goes twice across the shell it would be a two-tube pass heat exchanger. In Figure 2.7 a schematic of a five-shell passes and one-tube pass heat exchanger can be seen.

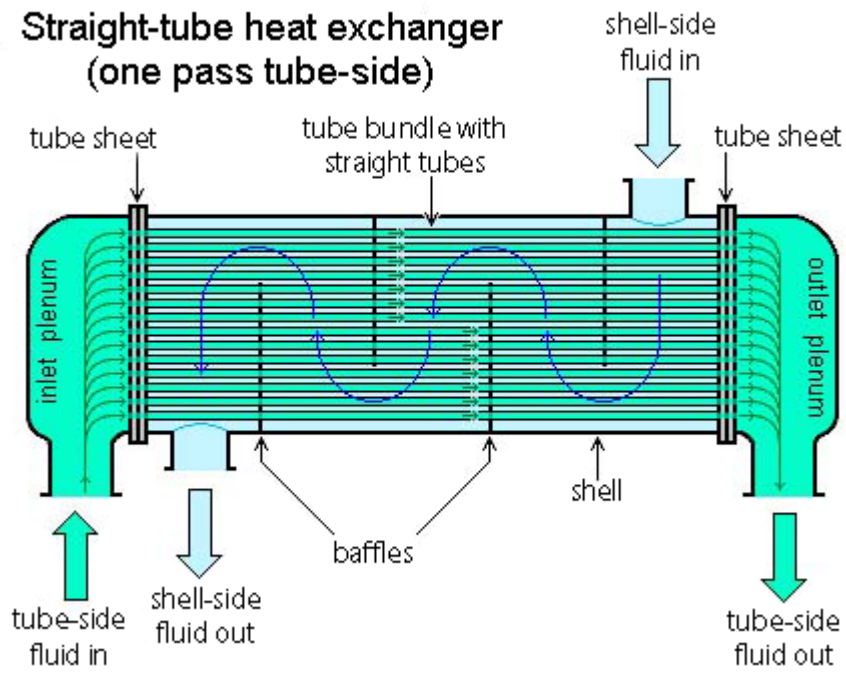

Figure 2.7: Shell-and-tube heat exchanger. The figure is from Wikipedia

2.2.2 Plate heat exchangers

The plate and frame heat exchanger consists of series of plates with corrugated flat flow passages which the fluid spreads over. The hot and cold fluids flow in alternate passages, that is, the cold fluid is surrounded by two hot fluid streams. The plates then transfer the heat between two fluids and the plates can also be used to induce turbulence in the flow at low flow speeds which enhances the heat transfer rate. It is a major advantage to have the chambers thin so that most of the fluids contact the plates. The heat transfer in plate heat exchangers can be extremely high because the chambers are thin, which ensures that a high portion of the fluids is in contact with the plates, and each stream of cold fluid is surrounded by two streams of hot fluid. Figure 2.8 shows a schematic of a plate heat exchanger and in the figure it can be seen how the plates are stacked together in a simple manner.

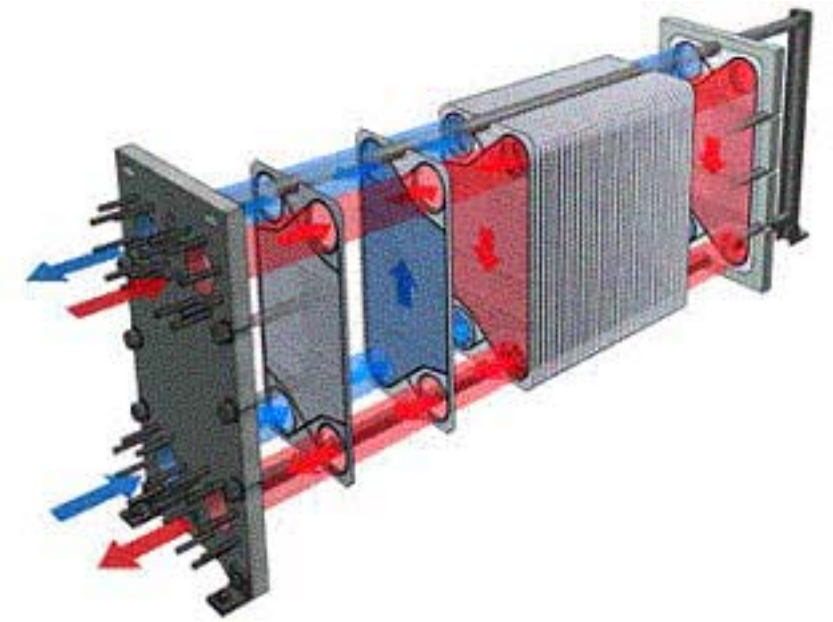

Figure 2.8: Plate heat exchanger, the figure is from Delta T Heat Exchangers, www.deltathx.com.

Plate heat exchangers can be either welded together or hold together with pressure. The choice between welded heat exchanger or not depends on the intended use.

A great advantage of the plate heat exchanger, if it is not welded together, over other types is that it is easy to expand or reduce the heat exchanger to the best size at each time. This is done simply by increasing or decreasing the number of plates in

the heat exchanger. Another advantage is how easily the plate heat exchanger can be dismantled for inspection and cleaning, and if single plates are damaged they can easily be replaced.

2.3 Common problems with heat exchangers

When using heat exchangers there are three well known fouling problems, which are [27, 33] and [20].

- Biological fouling will occur whenever a natural source of fluid is used, for example a lake water. Biological fouling can cause considerable damage when built up.
- Scale is another problem. Scale is chemical deposit layers such as calcium carbonate or magnesium carbonate. For instance when cooling water is heated during the cooling process dissolved salts in the fluid, for instance in geothermal water, will crystallize on the surface in the form of scale.
- Corrosion can be a problem in most heat exchanger. The problem can be solved partly by the type of material used in the heat exchanger. Heat exchangers made of stainless steel are usually the most corrosion resistant compared to heat exchangers made from other materials. When choosing the right heat exchanger, it should be observed in which kind of environment the heat exchanger operates. In geothermal powerplants the heat exchangers are sometimes made of titanium to resist corrosion.

As the fouling increases, the performance of the heat exchanger will deteriorate. The effect of fouling on the heat transfer is represented by a fouling factor, R_f, which is a measure of thermal resistance introduced by fouling. The fouling factor is a predetermined number that represents the amount of fouling a particular heat exchanger transferring a particular fluid will sustain.

According to [20] the most common way to account for the effects of fouling in heat exchangers is the application of the fouling factor. In the heat transfer equation the fouling factor is added to the other thermal resistances to calculate the Total Thermal Resistance which is the reciprocal of U for a clean heat exchanger. There are no direct calculations to determine the appropriate fouling factor to use for a given fluid in a particular application. However guidelines do exist to help determine an appropriate fouling factor. Typical values for the fouling factor can be found in [27] and are in the interval [0.0001, 0.0007].

Common ways to decrease the effect of fouling are, [6] and [2]:

- To maintain high level of turbulence in the flow, the turbulence will keep sediments from settling on the surface and also helps to clean off any existing fouling.
- To keep uniformly high velocities throughout the entire heat exchanger. High velocities will keep sediments from settling.
- To design the heat exchanger in a way that it can easily be cleaned.
- To oversize the heat exchanger to accommodate the effect of fouling. Care should be taken not to excessively oversize the heat exchanger because that might results in lower velocities of the fluids which in turn may promote fouling.
- Fluid treatment such as purification and addition of chemicals.

3 Theory

In this chapter the theory behind the work in the thesis is explained. It starts by giving a short introduction of the physics behind heat exchangers. Following the physics the mathematical models used in the thesis are derived. A short introduction to the Kalman filter follows. Finally a short description of the CuSum test will be given.

3.1 The Physics

Heat is energy. In thermodynamics there are 4 basic laws; the zeroth, first, second and third law, [6, 33]. This project focuses particularly on the first and second law.

- The **first law** of thermodynamics requires that the increase in the internal energy of a system is equal to the amount of energy added by heating the system, minus the amount removed as a result of the work done by the system on its surroundings.
- One consequence of the **second law** of thermodynamics is that heat is transferred in the direction of decreasing temperature, not the other way around.

Heat can be transferred by three phenomena; conduction, convection and radiation, [6].

- Conduction is the transfer of energy from the more energetic particles of a

substance to the adjacent less energetic ones as a result of interactions between the particles.

- Convection is the mode of energy transfer in a flowing fluid. It involves the combined effects of conduction and fluid motion. The faster the fluid motion, the greater the convection heat transfer.
- Radiation is the energy emitted by matter in the form of electromagnetic waves as a result of the changes in the electronic configurations of the atoms or molecules. Unlike conduction and convection, the transfer of energy by radiation does not require the presence of an intervening medium.

In heat exchangers the heat is transferred by convection (3.1) from the hot fluid to the separating metal and by conduction (3.2) through the metal and again by convection from the metal to the cold fluid. This involves:

$$q = -hA\Delta T \tag{3.1}$$

$$q = \frac{-kA}{\Delta x}\Delta T \tag{3.2}$$

where h is the convection heat transfer coefficient, A is the heat transfer area, ΔT is the temperature difference, k is the thermal conductivity and Δx is the thickness.

In this study a cross-flow heat exchanger is divided into ns sections on each side, see Figure 3.1. The arrows shown in the figure indicate the direction of the mass flow. The subscript ij indicates positions of a particular section, for instance $T_{h,11}$ is the section in the upper left corner on the hot side. The energy can only travel with the mass flow and trough the heat exchanger to the corresponding section in the cold part; i.e. energy in section $T_{h,11}$ can only flow to $T_{h,21}$ and $T_{c,21}$

In this study the following assumptions are used:

1. The heat exchanger is perfectly insulated. That is, the heat loss to the surroundings is negligible.
2. There is no heat conduction in the direction of the flow in the metal between the fluids or in the fluids themselves.
3. There is uniform temperature in each section of the heat exchanger.
4. The specific heat capacities are constant through the heat exchanger.

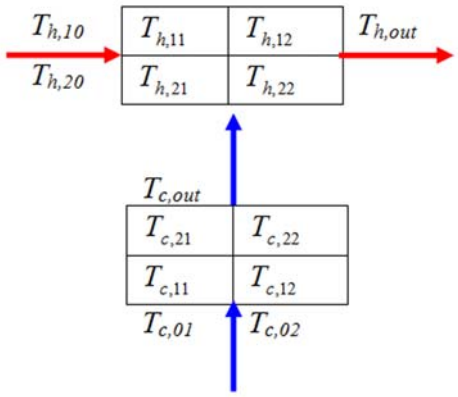

Figure 3.1: Cross-flow heat exchanger with 4 sections on each side

Using the above assumptions the differential energy balance equation (3.3) is derived for each section of the heat exchanger.

$$\underbrace{Mc\frac{dT_{ij}(t)}{dt}}_{i} = \underbrace{\dot{m}(t)c[T_{i-nj-m}(t) - T_{ij}(t)]}_{ii} \pm \underbrace{AU_{ij}(t)\Delta T_{ij}(t)}_{iii} \tag{3.3}$$

where:

- i) is the energy change in section ij at a given time t.
- ii) is the energy flow in the fluid in section ij. Were $n = 1$ and $m = 0$ for the cold side, and $n = 0$ and $m = 1$ for the hot side.
- iii) is the energy that is transferred from or to section ij. A positive sign for the cold side and negative sign for the hot side.

It could be possible to add new terms to the equation. For example the energy loss to the surroundings. The energy loss to the surroundings would be represented by another heat transfer term, $A_sU_s(t)\Delta T_s(t)$, on the right side of (3.3), but it is not done here because here it is assumed that the energy loss to the surroundings is negligible.

It is also possible to model the effect of the metal between the fluids. In [14] it is shown for a similar model for counter-flow heat exchanger that adding the effect of the metal to to the model does not add significantly to the accuracy of the model.

3.2 The model

In this section the following will be given:

- Mathematical model for a cross-flow heat exchanger.
- Empirical relations in the model.
- Explanation about the parameter estimation.
- Expansion of the model to the **on-line method**.

When deriving the mathematical model the assumptions stated in Chapter 3 are used. Figure 3.1 shows a schematic layout of the model.

3.2.1 Mathematical state space model

The following energy balance equations are found by implementing (3.3) for each section in the hot and cold side respectively.

$$M_h c_h \frac{dT_{h,ij}(t)}{dt} = \dot{m}_h(t) c_h [T_{h,ij-1}(t) - T_{h,ij}(t)] - A_h U_{ij}(t) F \Delta T_{ij}(t) \tag{3.4}$$

$$M_c c_c \frac{dT_{c,ij}(t)}{dt} = \dot{m}_c(t) c_c [T_{c,i-1j}(t) - T_{c,ij}(t)] + A_c U_{ij}(t) F \Delta T_{ij}(t) \tag{3.5}$$

where $i = 1, ..., n$ and $j = 1, ..., s$.

The temperature of the fluids decreases/increases as the fluid goes through the cells and $\Delta T_{ij}(t)$ is the temperature difference between the cells ij and the corresponding cell on the other side of the heat exchanger. For the cross-flow heat exchanger [6] recommends to use the representation of $\Delta T_{ij}(t)$ for the counter-flow heat exchanger with a correction factor F. The correction factor depends on the geometry of the cross-flow heat exchanger and the inlet and outlet temperatures of the hot and cold fluid streams. The correction factor F has a value less tan or equal to 1, where the case $F = 1$ corresponds to the counter-flow heat exchanger. Tables for F can be seen in [6].

There are several ways to represent $\Delta T_{ij}(t)$.

1. The most simple would be to take the temperature difference of the two cells,

$$\Delta T_{ij}(t) = T_{h,ij}(t) - T_{c,ij}(t) \tag{3.6}$$

2. More accurate would be to use the arithmetic mean temperature in cells,

$$\Delta T_{ij}(t) = [T_{h,ij-1}(t) + T_{h,ij}(t)]/2 - [T_{c,i-1j}(t) + T_{c,ij}(t)]/2 \tag{3.7}$$

3. The most accurate way is to use the log mean temperature difference,

$$\Delta T_{ij}(t) = \frac{[T_{h,ij-1}(t) - T_{c,ij}(t)] - [T_{h,ij}(t) - T_{c,i-1j}(t)]}{ln([[T_{h,ij-1}(t) - T_{c,ij}(t)]/[T_{h,ij}(t) - T_{c,i-1j}(t)]} \tag{3.8}$$

In [14] it is suggested to use representation 2 since representation 3 will introduce extra nonlinearities in the model.

By introducing the following parameters:

$$\alpha_{ij}(t) = \frac{FA_hU_{ij}(t)}{\dot{m}_h(t)c_h} \tag{3.9}$$

$$\beta_{ij}(t) = \frac{FA_cU_{ij}(t)}{\dot{m}_c(t)c_c} \tag{3.10}$$

$$\tau_h(t) = \frac{M_h}{\dot{m}_h(t)} \tag{3.11}$$

$$\tau_c(t) = \frac{M_c}{\dot{m}_c(t)} \tag{3.12}$$

and by inserting (3.9), (3.10), (3.11), (3.12) and (3.7) into (3.4) and (3.5) the model equations for the hot and cold side respectively become:

$$\frac{dT_{h,ij}(t)}{dt} = (1-\frac{\alpha_{ij}}{2})\tau_h^{-1}T_{h,ij-1}(t)-(1+\frac{\alpha_{ij}}{2})\tau_h^{-1}T_{h,ij}(t)+(\frac{\alpha_{ij}}{2\tau_h})T_{c,i-1j}(t)+(\frac{\alpha_{ij}}{2\tau_h})T_{c,ij}(t) \tag{3.13}$$

$$\frac{dT_{c,ij}(t)}{dt} = (1-\frac{\beta_{ij}}{2})\tau_c^{-1}T_{c,i-1j}(t)-(1+\frac{\beta_{ij}}{2})\tau_c^{-1}T_{c,ij}(t)+(\frac{\beta_{ij}}{2\tau_c})T_{h,ij-1}(t)+(\frac{\beta_{ij}}{2\tau_c})T_{h,ij}(t) \tag{3.14}$$

Equations (3.13) and (3.14) can be written in state space form as

$$\frac{d}{dt}\underline{T} = \mathbf{A}(\underline{\dot{m}},\underline{\theta})\underline{T} + \mathbf{B}(\underline{\dot{m}},\underline{\theta})\underline{T_{in}} \tag{3.15}$$

and in matrix from it will be

$$\frac{d}{dt}\begin{bmatrix} T_{h,11} \\ T_{h,12} \\ T_{h,21} \\ T_{h,22} \\ T_{c,11} \\ T_{c,12} \\ T_{c,21} \\ T_{c,22} \end{bmatrix} = \begin{bmatrix} \frac{-(1+\frac{\alpha_{11}}{2})}{\tau_h} & 0 & 0 & 0 & \frac{\alpha_{11}}{2\tau_h} & 0 & 0 & 0 \\ \frac{(1-\frac{\alpha_{12}}{2})}{\tau_h} & \frac{-(1+\frac{\alpha_{12}}{2})}{\tau_h} & 0 & 0 & 0 & \frac{\alpha_{12}}{2\tau_h} & 0 & 0 \\ 0 & 0 & \frac{-(1+\frac{\alpha_{21}}{2})}{\tau_h} & 0 & \frac{\alpha_{21}}{2\tau_h} & 0 & \frac{\alpha_{21}}{2\tau_h} & 0 \\ 0 & 0 & \frac{(1-\frac{\alpha_{22}}{2})}{\tau_h} & \frac{-(1+\frac{\alpha_{22}}{2})}{\tau_h} & 0 & \frac{\alpha_{22}}{2\tau_h} & 0 & \frac{\alpha_{22}}{2\tau_h} \\ \frac{\beta_{11}}{2\tau_c} & 0 & 0 & 0 & \frac{-(1+\frac{\beta_{11}}{2})}{\tau_c} & 0 & 0 & 0 \\ \frac{\beta_{12}}{2\tau_c} & \frac{\beta_{12}}{2\tau_c} & 0 & 0 & 0 & \frac{-(1+\frac{\beta_{12}}{2})}{\tau_c} & 0 & 0 \\ 0 & 0 & \frac{\beta_{21}}{2\tau_c} & 0 & \frac{(1-\frac{\beta_{21}}{2})}{\tau_c} & 0 & \frac{-(1+\frac{\beta_{31}}{2})}{\tau_c} & 0 \\ 0 & 0 & \frac{\beta_{22}}{2\tau_c} & \frac{\beta_{22}}{2\tau_c} & 0 & \frac{(1-\frac{\beta_{22}}{2})}{\tau_c} & 0 & \frac{-(1+\frac{\beta_{22}}{2})}{\tau_c} \end{bmatrix} \begin{bmatrix} T_{h,11} \\ T_{h,12} \\ T_{h,21} \\ T_{h,22} \\ T_{c,11} \\ T_{c,12} \\ T_{c,21} \\ T_{c,22} \end{bmatrix}$$

$$+ \begin{bmatrix} \frac{(1-\frac{\alpha_{11}}{2})}{\tau_h} & 0 & \frac{\alpha_{11}}{2\tau_h} & 0 \\ 0 & 0 & 0 & \frac{\alpha_{12}}{2\tau_h} \\ 0 & \frac{(1-\frac{\alpha_{21}}{2})}{\tau_h} & 0 & 0 \\ 0 & 0 & 0 & 0 \\ \frac{\beta_{11}}{2\tau_c} & 0 & \frac{(1-\frac{\beta_{11}}{2})}{\tau_c} & 0 \\ 0 & 0 & 0 & \frac{(1-\frac{\beta_{12}}{2})}{\tau_c} \\ 0 & \frac{\beta_{21}}{2\tau_c} & 0 & 0 \\ 0 & 0 & 0 & 0 \end{bmatrix} \begin{bmatrix} T_{h,10} \\ T_{h,20} \\ T_{c,01} \\ T_{c,02} \end{bmatrix} \tag{3.16}$$

The outlet temperature are calculated with:

$$T_{out} = \begin{bmatrix} 0 & 0.5 & 0 & 0.5 & 0 & 0 & 0 & 0 \\ 0 & 0 & 0 & 0 & 0 & 0 & 0.5 & 0.5 \end{bmatrix} \begin{bmatrix} T_{h,11} \\ T_{h,12} \\ T_{h,21} \\ T_{h,22} \\ T_{c,11} \\ T_{c,12} \\ T_{c,21} \\ T_{c,22} \end{bmatrix} \tag{3.17}$$

It is easy to increase the number of section on each side in this model. But the size of the **A** matrix will always be double the number of the section on each side. That is if there are 9 sections on each side **A** will be 18x18 matrix.

3.2.2 Empirical relations in the model parameters

In [15] empirical relations of the heat transfer coefficient are incorporated in the parameters in a heat exchanger model. The coefficient is then estimated along with

the parameters over the operating area of the heat exchanger. By using the empirical relations it is possible, according to [15], to use a very low model order.

Since the model derived is a mass dependent model, it is assumed that the convection coefficient, h, is a function of the mass flow, [15].

$$h(t) = C'\dot{m}^y(t) \tag{3.18}$$

[15].

It is assumed that the thermal resistance in the metal is negligible. This is a reasonable assumption since the separating metal is usually thin and has high thermal conductivity.

The overall heat transfer coefficient, U, is a function of the heat coefficients with following relation.

$$U^{-1} = \frac{1}{h_h} + \frac{1}{h_c} \tag{3.19}$$

By assuming that (3.18) applies to both of the heat transfer coefficients, h_h and h_c, the overall heat transfer coefficient U, is given by

$$U(t) = \frac{h_h h_c}{h_h(t) + h_c(t)} = \frac{C'(\dot{m}_h(t)\dot{m}_c(t))^y}{(\dot{m}_h^y(t) + \dot{m}_c^y(t))} \tag{3.20}$$

In [15] it is pointed out that since the mass flow is present in the denominator in all of the model parameters it is practical to normalize them by some reference mass flow $\dot{m}_{ref}$. Since U is also mass flow dependent the parameters α and β are also normalized with U_{ref}, (3.21).

The overall heat transfer coefficient according to the reference mass flow $\dot{m}_{h*}$ and $\dot{m}_{c*}$ is similarly

$$U_{ref} = \frac{h_{h*} h_{c*}}{h_{c*} + h_{c*}} = \frac{C'(\dot{m}_{h*}\dot{m}_{c*})^y}{(\dot{m}_{h*}^y + \dot{m}_{c*}^y)} \tag{3.21}$$

After normalizing the parameters they become

$$\alpha_{ij}(t) = \alpha_{ij*}\frac{\dot{m}_{h*}}{\dot{m}_h(t)}\frac{U_{ij}(t)}{U_{ij*}} \tag{3.22}$$

$$\beta_{ij}(t) = \beta_{ij*}\frac{\dot{m}_{c*}}{\dot{m}_c(t)}\frac{U_{ij}(t)}{U_{ij*}} \tag{3.23}$$

$$\tau_h(t) = \tau_{h*}\frac{\dot{m}_{h*}}{\dot{m}_h(t)} \tag{3.24}$$

$$\tau_c(t) = \tau_{c*}\frac{\dot{m}_{c*}}{\dot{m}_c(t)} \tag{3.25}$$

where α_{ij*}, β_{ij*}, τ_{h*}, τ_{c*} are from equations (3.9), (3.10), (3.11) and (3.12) respectively.

The parameters in (3.22), (3.23), (3.24) and (3.25) along with the exponent y in (3.20) and (3.21) form the parameter set in the heat exchanger model.

3.2.3 The detection of fouling

When fouling accumulates in a heat exchanger the resistance to heat transfer increases, which decreases the overall heat transfer coefficient U. It can be hard to detect changes in U in heat exchangers with frequent mass flow changes since the overall heat transfer coefficient is correlated with the mass flow through the Reynolds number as can be seen in (3.26), [6].

$$U = \frac{1}{\frac{1}{A_c h_c} + \frac{1}{A_h h_h}}/WH \tag{3.26}$$

where

$$h_i = \frac{Nu_i k_i}{Dh_i}$$

$$Nu_i = 0.023 Re_i^y Pr_i^{\frac{1}{3}}$$

$$Re_i = \frac{\dot{m}_i Dh_i}{\rho H d_i \nu_i}$$

Where $i = h, c$ indicates the subscripts for either the cold or the hot side.

Since it is not possible to observe U directly, is is observed indirectly through the parameters α and β. By looking on (3.9) and (3.10) it can be seen that if U decreases the α and β will also decrease. With this connection to U it is possible to detect

fouling through a shift in the parameters α and β. The shift is detected with CuSum chart, see Section 3.5.

3.2.4 The off-line method

The heat exchanger model presented in (3.15) is deterministic. To compensate for deviations from the correct temperature values it is necessary to add a noise term, $w_\theta(t)$, to the model, where $w_\theta(t) \in N(0, Q_\theta(t))$ i.e. independent normal distributed white noise process with zero mean. The general form becomes.

$$\frac{d}{dt}\underline{T} = \mathbf{A}(\underline{\dot{m}}, \underline{T}, \underline{\theta})\underline{T} + \mathbf{B}(\underline{\dot{m}}, \underline{T}, \underline{\theta})\underline{T_{in}} + \underline{w}_f(t) = \underline{f}(\underline{\dot{m}}, \underline{T}, \underline{\theta}, \underline{T_{in}}) + \underline{w}_f(t)$$

Since the model used in this study is continuous it needs to be made discrete before the standard Kalman filter can be used to estimate the states. By assuming that the temperature and mass flows are constant between sampling instants it is possible to write the model in discrete time.

$$\underline{T}(t + \Delta t) = \Phi(\underline{\dot{m}}, \Delta t)\underline{T}(t) + \Gamma(\underline{\dot{m}}, \Delta t)\underline{T}_{in}(t) + w(t + \Delta t) \tag{3.27}$$

where

$$\Phi(\underline{\dot{m}}, \Delta t) = e^{\mathbf{A}(\underline{\dot{m}})} = \sum_{i=1}^{\infty} \frac{\mathbf{A}(\underline{\dot{m}})^i}{i!} \tag{3.28}$$

and

$$\Gamma(\underline{\dot{m}}, \Delta t) = [\int_0^{\Delta t} e^{\mathbf{A}(\underline{\dot{m}})s} ds]\mathbf{B}(\underline{\dot{m}}) \tag{3.29}$$

$w(t + \Delta t)$ is a white noise with zero mean and covariance $Q(t)$. The covariance should be a function of the sampling interval and the mass flow, but in this case the sampling time is constant and to simplify, the mass flow dependence is neglected. As is mentioned above the standard Kalman filter, see Section 3.4, is used to estimate the states in the model which is not possible to measure, that is the temperatures in the sections of the heat exchanger. The parameters of the model, $\underline{\theta}$, are then estimated with the method of least squares, [22].

The aim is to find the values of the parameters in the vector $\underline{\theta}$ that minimizes the score function (3.30), where the score function is the sum of the squares of the deviations of the observations from the true regression line. In (3.30) t_1 represents the start

of the time series which is being investigated. The aim is therefore to minimize the score function from time t_1 to t_N.

$$V(\underline{\theta}) = \sum_{t=t_1}^{N} \varepsilon(t)^T \varepsilon(t) \tag{3.30}$$

If the heat exchanger is modeled with 4 sections and two mass flows on each side, see Figure 3.1, the expected values of parameters can be calculated from (3.9), (3.10), (3.11), (3.12) and (3.26) for a given mass flow if the dimensions of the heat exchanger are known.

In the analysis it is assumed that the flow in the heat exchanger is a fully developed turbulent flow. In the case of a fully developed turbulent flow the literature recommends to use $y = 0.8$, [6].

The downside of this method of estimating the parameters is that it needs much activity in the data to be able to estimate the parameters. This method might not be the best method for detecting the parameters in the case of a steady state heat exchanger.

3.2.5 The on-line method

In [16] a similar method is used for counter-flow heat exchanger. By letting α^* and β^* be model states it is possible to observe the changes in U on-line. This is done by adding two new differential equations to the heat exchanger model in (3.15). α^* and β^* are described as purely random processes.

$$\frac{d}{dt}\begin{bmatrix} \alpha^*(t) \\ \beta^*(t) \end{bmatrix} = \frac{d}{dt}[\underline{\theta}] = \underline{w}_\theta(t) \tag{3.31}$$

where $\underline{w}_\theta(t) \in N(0, Q_\theta(t))$, i.e. independent normal distributed white noise process with zero mean.

After expanding the model (3.15) with (3.31) it becomes

$$\frac{d}{dt}\begin{bmatrix} \underline{\theta} \\ \underline{T} \end{bmatrix} = \begin{bmatrix} \underline{0} \\ \underline{f}(\underline{\dot{m}}, \underline{T}, \underline{\theta}, \underline{T_{in}}) \end{bmatrix} + \begin{bmatrix} \underline{w}_\theta \\ \underline{w}_f \end{bmatrix} \tag{3.32}$$

Here $\underline{w}_f = N(0, Q_f)$ has been added to (3.15) to compensate for deviations from the correct temperature values.

Since the model is continuous in time and the measurements are discrete the Extended Kalman filter is used to estimate the states of the model. The extended Kalman filter is based on linearization around the current state estimates, $\hat{T}$, see Section 3.4. The continuous- discrete version of the extended Kalman filter is quite similar to the standard discrete Kalman filter. The main difference is that the state vector and the covariance matrix can not be propagated in the same manner due to nonlinearity in the model, therefore the following equations are used for state estimation propagation and error covariance propagation respectively.

$$\frac{d}{dt}\underline{\hat{T}}(t) = f(\underline{\hat{x}}(t)) \tag{3.33}$$

$$\frac{d}{dt}\mathbf{P}(t) = \mathbf{F}(\underline{\hat{x}}(t))\mathbf{P}(t) + \mathbf{P}(t)\mathbf{F}^T(\underline{\hat{x}}(t), t) + \mathbf{Q}(t) \tag{3.34}$$

where

$$F(\underline{\hat{x}}(t)) = \frac{\partial \begin{bmatrix} \underline{0} \\ \underline{f}(\underline{\dot{m}}, \underline{T}, \underline{\theta}, \underline{T_{in}}) \end{bmatrix}}{\partial \underline{x}} | (\underline{x}(t) = \underline{\hat{x}}(t)) \tag{3.35}$$

The values of F are the derivatives of the model equations with respect to the model parameters. The model equations are shown in (3.36).

$$\frac{d}{dt}\begin{bmatrix} \alpha^*(t) \\ \beta^*(t) \\ T_{h,11} \\ T_{h,12} \\ T_{h,21} \\ T_{h,22} \\ T_{c,11} \\ T_{c,12} \\ T_{c,21} \\ T_{c,22} \end{bmatrix} = \begin{bmatrix} 0 \\ 0 \\ -\frac{(1+\frac{\alpha_{11}}{2})}{\tau_h}T_{h,11} + \frac{\alpha_{11}}{2\tau_h}T_{c,11} + \frac{(1-\frac{\alpha_{11}}{2})}{\tau_h}T_{h,10} + \frac{\alpha_{11}}{2\tau_h}T_{c,01} \\ \frac{(1-\frac{\alpha_{12}}{2})}{\tau_h}T_{h,11} - \frac{(1+\frac{\alpha_{12}}{2})}{\tau_h}T_{h,12} + \frac{\alpha_{12}}{2\tau_h}T_{c,12} + \frac{\alpha_{12}}{2\tau_h}T_{c,02} \\ -\frac{(1+\frac{\alpha_{21}}{2})}{\tau_h}T_{h,21} + \frac{\alpha_{21}}{2\tau_h}T_{c,11} + \frac{\alpha_{21}}{2\tau_h}T_{c,21} + \frac{(1-\frac{\alpha_{21}}{2})}{\tau_h}T_{h,20} \\ \frac{(1-\frac{\alpha_{22}}{2})}{\tau_h}T_{h,21} - \frac{(1+\frac{\alpha_{22}}{2})}{\tau_h}T_{h,22} + \frac{\alpha_{22}}{2\tau_h}T_{c,12} + \frac{\alpha_{22}}{2\tau_h}T_{c,22} \\ \frac{\beta_{11}}{2\tau_c}T_{h,11} - \frac{(1+\frac{\beta_{11}}{2})}{\tau_c}T_{c,11} + \frac{\beta_{11}}{2\tau_c}T_{h,10} + \frac{(1-\frac{\beta_{11}}{2})}{\tau_c}T_{c,01} \\ \frac{\beta_{12}}{2\tau_c}T_{h,11} + \frac{\beta_{12}}{2\tau_c}T_{h,12} - \frac{(1+\frac{\beta_{12}}{2})}{\tau_c}T_{c,12} + \frac{(1-\frac{\beta_{12}}{2})}{\tau_c}T_{c,02} \\ \frac{\beta_{21}}{2\tau_c}T_{h,21} + \frac{(1-\frac{\beta_{21}}{2})}{\tau_c}T_{c,11} - \frac{(1+\frac{\beta_{21}}{2})}{\tau_c}T_{c,21} + \frac{\beta_{21}}{2\tau_c}T_{h,20} \\ \frac{\beta_{22}}{2\tau_c}T_{h,21} + \frac{\beta_{22}}{2\tau_c}T_{h,22} + \frac{(1-\frac{\beta_{22}}{2})}{\tau_c}T_{c,12} - \frac{(1+\frac{\beta_{22}}{2})}{\tau_c}T_{c,22} \end{bmatrix} + \begin{bmatrix} \underline{w}_\theta \\ \underline{w}_f \end{bmatrix}$$

$$= \begin{bmatrix} 0 \\ 0 \\ f_1 \\ f_2 \\ f_3 \\ f_4 \\ f_5 \\ f_6 \\ f_7 \\ f_8 \end{bmatrix} + \begin{bmatrix} \underline{w}_\theta \\ \underline{w}_f \end{bmatrix} \tag{3.36}$$

From here on the following assumptions are used unless otherwise stated:

- All the cells on the hot side have the same α.
- All the cells on the cold side have the same β.

In matrix form F will therefore become the following 10 by 10 matrix.

$$F = \begin{bmatrix} 0 & 0 & 0 & 0 & 0 & 0 & 0 & 0 & 0 & 0 \\ 0 & 0 & 0 & 0 & 0 & 0 & 0 & 0 & 0 & 0 \\ \frac{\partial f_1}{d\alpha} & \frac{\partial f_1}{d\beta} & \frac{\partial f_1}{dT_{h,11}} & \frac{\partial f_1}{dT_{h,12}} & \frac{\partial f_1}{dT_{h,21}} & \frac{\partial f_1}{dT_{h,22}} & \frac{\partial f_1}{dT_{c,11}} & \frac{\partial f_1}{dT_{c,12}} & \frac{\partial f_1}{dT_{c,21}} & \frac{\partial f_1}{dT_{c,22}} \\ \frac{\partial f_2}{d\alpha} & \frac{\partial f_2}{d\beta} & \frac{\partial f_2}{dT_{h,11}} & \frac{\partial f_2}{dT_{h,12}} & \frac{\partial f_2}{dT_{h,21}} & \frac{\partial f_2}{dT_{h,22}} & \frac{\partial f_2}{dT_{c,11}} & \frac{\partial f_2}{dT_{c,12}} & \frac{\partial f_2}{dT_{c,21}} & \frac{\partial f_2}{dT_{c,22}} \\ \frac{\partial f_3}{d\alpha} & \frac{\partial f_3}{d\beta} & \frac{\partial f_3}{dT_{h,11}} & \frac{\partial f_3}{dT_{h,12}} & \frac{\partial f_3}{dT_{h,21}} & \frac{\partial f_3}{dT_{h,22}} & \frac{\partial f_3}{dT_{c,11}} & \frac{\partial f_3}{dT_{c,12}} & \frac{\partial f_3}{dT_{c,21}} & \frac{\partial f_3}{dT_{c,22}} \\ \frac{\partial f_4}{d\alpha} & \frac{\partial f_4}{d\beta} & \frac{\partial f_4}{dT_{h,11}} & \frac{\partial f_4}{dT_{h,12}} & \frac{\partial f_4}{dT_{h,21}} & \frac{\partial f_4}{dT_{h,22}} & \frac{\partial f_4}{dT_{c,11}} & \frac{\partial f_4}{dT_{c,12}} & \frac{\partial f_4}{dT_{c,21}} & \frac{\partial f_4}{dT_{c,22}} \\ \frac{\partial f_5}{d\alpha} & \frac{\partial f_5}{d\beta} & \frac{\partial f_5}{dT_{h,11}} & \frac{\partial f_5}{dT_{h,12}} & \frac{\partial f_5}{dT_{h,21}} & \frac{\partial f_5}{dT_{h,22}} & \frac{\partial f_5}{dT_{c,11}} & \frac{\partial f_5}{dT_{c,12}} & \frac{\partial f_5}{dT_{c,21}} & \frac{\partial f_5}{dT_{c,22}} \\ \frac{\partial f_6}{d\alpha} & \frac{\partial f_6}{d\beta} & \frac{\partial f_6}{dT_{h,11}} & \frac{\partial f_6}{dT_{h,12}} & \frac{\partial f_6}{dT_{h,21}} & \frac{\partial f_6}{dT_{h,22}} & \frac{\partial f_6}{dT_{c,11}} & \frac{\partial f_6}{dT_{c,12}} & \frac{\partial f_6}{dT_{c,21}} & \frac{\partial f_6}{dT_{c,22}} \\ \frac{\partial f_7}{d\alpha} & \frac{\partial f_7}{d\beta} & \frac{\partial f_7}{dT_{h,11}} & \frac{\partial f_7}{dT_{h,12}} & \frac{\partial f_7}{dT_{h,21}} & \frac{\partial f_7}{dT_{h,22}} & \frac{\partial f_7}{dT_{c,11}} & \frac{\partial f_7}{dT_{c,12}} & \frac{\partial f_7}{dT_{c,21}} & \frac{\partial f_7}{dT_{c,22}} \\ \frac{\partial f_8}{d\alpha} & \frac{\partial f_8}{d\beta} & \frac{\partial f_8}{dT_{h,11}} & \frac{\partial f_8}{dT_{h,12}} & \frac{\partial f_8}{dT_{h,21}} & \frac{\partial f_8}{dT_{h,22}} & \frac{\partial f_8}{dT_{c,11}} & \frac{\partial f_8}{dT_{c,12}} & \frac{\partial f_8}{dT_{c,21}} & \frac{\partial f_8}{dT_{c,22}} \end{bmatrix} \tag{3.37}$$

3.3 The slope method

If the heat exchanger being investigated operates in a condition close to a steady state the methods discussed in previous chapters might not work since they need

frequent variations in the inputs to estimate the parameters of the model. The following method is specially designed to monitor heat exchangers that are almost in a steady state operation. For instance the heat exchangers used in the district heating industry. According to the energy company Hitaveita Suðurnesja the heat exchangers used there are usually close to a steady state operation their whole operating time. The heat exchangers get hot steam with almost constant pressure and flow. The cold side usually has almost constant temperature, but the cold mass flow can have some variations.

The method uses the following assumptions:

- Steady operating conditions exist.
- Changes in the kinetic and potential energies of fluid streams are negligible.
- Fluid properties are constant.

The heat transfer rate for a parallel-flow and counter-flow heat exchanger in a steady state is

$$\dot{Q} = UA\Delta T_{LMTD} = \dot{m}_k c_p \Delta T_k \tag{3.38}$$

where the subscript k indicates either the hot or the cold side.

For a cross-flow heat exchanger it is necessary to add a correction factor F for the log mean temperature difference, ΔT_{LMTD}. The value of F can be found in tables in [6]. By looking on (3.38) the following relation can be derived $\dot{m}\Delta T \propto UAF\Delta T_{LMTD}$.

This method finds the fouling by calculating the slope AUF over a sliding window of size N from the plot $\dot{m}\Delta T$ against ΔT_{LMTD}. A typical plot can be seen in Figure 3.2. By viewing the figure it can clearly be seen that there are strong correlations between observations. By monitoring the slope for changes from the slope of a reference operation it is possible to find out when the heat exchanger starts to build up fouling. As the slope decreases the more fouled the heat exchanger is. Because of the correlations it is necessary to have relatively long windows when estimating the slopes to minimize the effect of the correlations, especially when estimating the reference slope because the detection is done by comparing how the slope is changing with time to the reference slope.

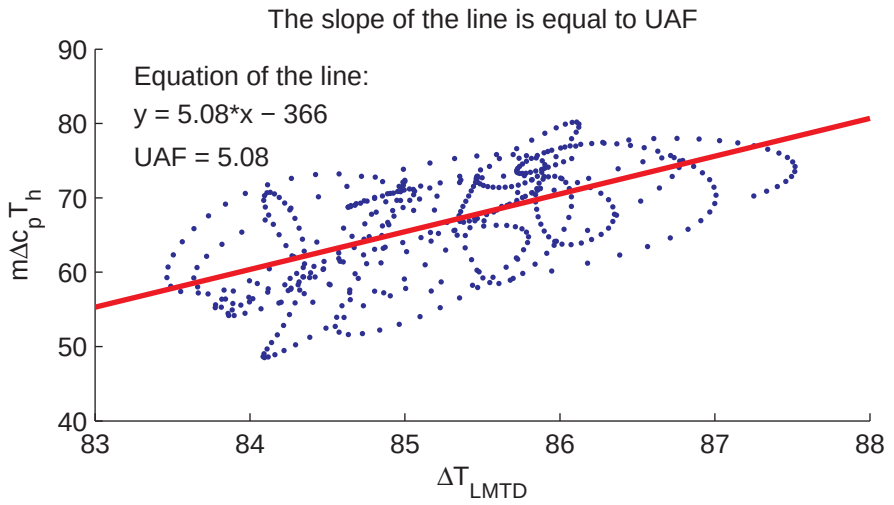

Figure 3.2: The figure shows a typical plot of $\dot{m}c_p\Delta T$ against ΔT_{LMTD} for one window.

3.4 Kalman filter

The following is a short introduction to the Kalman filter, [4, 19, 32] and [21].

The Kalman filter was first published in 1960 by R.E. Kalman, since than the Kalman filter has been a subject of extensive research and application. The filter is a multiple-input, multiple-output recursive filter that is used to estimate the state of a noisy process by implementing a set of mathematical equations. The filter is very powerful in several aspects: it supports estimations of past, present and futures states. The filter can be used to estimates states even when the precise nature of the modeled system is unknown, [32]. The filter assumes that the noise in the measurements is Gaussian white noise with mean value 0. The Kalman filter filters the noisy measurements that are given to it to estimate the desired state. The estimates are statistically optimal in the sense that they minimize the mean-square estimation error.

It can be seen when inspecting (3.39) to (3.43) and (3.44) to (3.48) that when a new observation is given the Kalman filter does not look directly on any previous observation, since it stores the information from all the earlier observations in the previous best estimate and its covariance matrix. This is a key factor since it means that the Kalman filter is not doing any more work when calculating the millionth estimate than it does for the first estimate.

The Kalman filter is used to estimate the states in a given model that are not possible

to measure. In this study the Kalman filter is used to estimate the temperatures inside the heat exchanger and in the on-line method it is also used to estimate the parameters α and β of the model.

3.4.1 Standard Kalman filter

The standard Kalman filter is an algorithm to estimate states in discrete time and consists of the following mathematical equations, and is applied in the following order recursively:

1. Set initial estimates
2. Project the state ahead:

$$\hat{x}_k^- = A\hat{x}_{k-1} + Bu_{k-1} \tag{3.39}$$

3. Project the error covariance ahead

$$P_k^- = AP_{k-1}A^T + Q \tag{3.40}$$

4. Compute the Kalman gain

$$K_k = P_k^- H^T (HP_k^- H^T + R)^{-1} \tag{3.41}$$

5. Update estimate with measurement z_k

$$\hat{x}_k = \hat{x}_k^- + K_k(z_k - H\hat{x}_k^-) \tag{3.42}$$

6. Update the error covariance

$$P_k = (I - K_k H)P_k^- \tag{3.43}$$

7. Repeat steps 2 to 6 for the next time step, see figure 3.3.

3.4.2 Extended Kalman filter, EKF

If the process that is to be estimated is non-linear, the EKF should be used. The EKF linearizes around the current mean and covariance. The EKF consists of the following mathematical equations and is applied in the following order recursively:

1. Set initial estimates
2. Project the state ahead:

$$\hat{x}_k^- = f(\hat{x}_{k-1}, u_{k-1}, 0) \tag{3.44}$$

3. Project the error covariance ahead

$$P_k^- = A_k P_{k-1} A_k^T + W_k Q_{k-1} W_k^T \tag{3.45}$$

4. Compute the Kalman gain

$$K_k = P_k^- H_k^T (H_k P_k^- H_k^T + V_k R_k V_k^T)^{-1} \tag{3.46}$$

5. Update estimate with measurement z_k

$$\hat{x}_k = \hat{x}_k^- + K_k(z_k - h(\hat{x}_k^-, 0)) \tag{3.47}$$

6. Update the error covariance

$$P_k = (I - K_k H_k) P_k^- \tag{3.48}$$

7. Repeat steps 2 to 6 for the next time step, see figure 3.4.

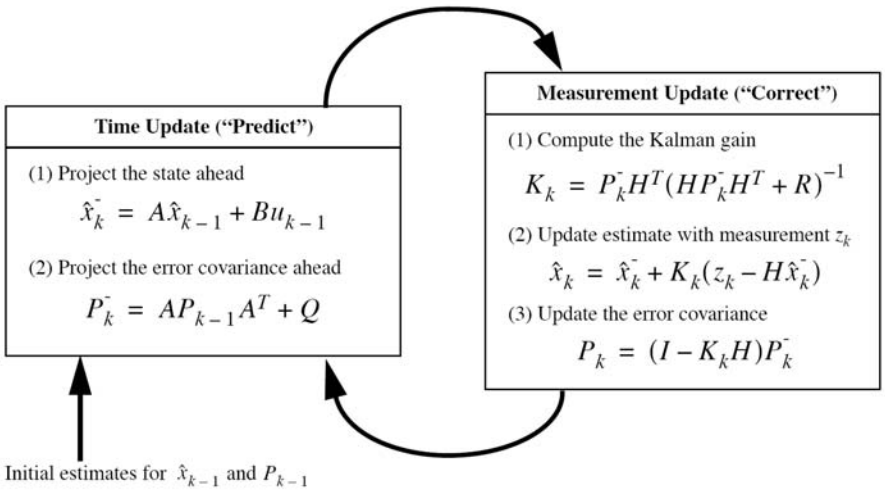

Figure 3.3: Estimation process of the standard Kalman filter, the left box is the propagation and the right box is the update process

3.5 Cumulative sum control chart

According to [26] the Cumulative sum control chart (CuSum) is very efficient when detecting small shift in mean of a process. Thus is the CuSum chart is used in this study.

A result of fouling in heat exchangers is a decrease in the overall heat transfer coefficient, U. Since the parameters in the models depend on U the progress of fouling can be monitored through them. It can be seen in (3.26) that U is mass dependent. Since the parameters of the models depend on U they change also with the mass flow. Due to the mass dependency it can be difficult to detect when fouling has begun in heat exchangers where the mass flow changes frequently. In those cases the ability of the CuSum chart to detect small shifts in mean values is really good.

When analyzing the parameters the average value of the parameters is calculated over a window of a specific length, which is chosen in accordance with the process being studied, and the CuSum chart is used to monitor the average value of the parameters for a shift from their reference value. If the average is not changing in time it is said to be under control, if on the other hand there is a shift in the average it is said to be out of control. If the process remains in control the cumulative sum should fluctuate around zero. If there is a shift in the value of the parameters, either upwards or downwards, the CuSum chart should pick it up quickly. If there is an upward shifting it is said to be a positive shift and conversely if there is a downward shift in the

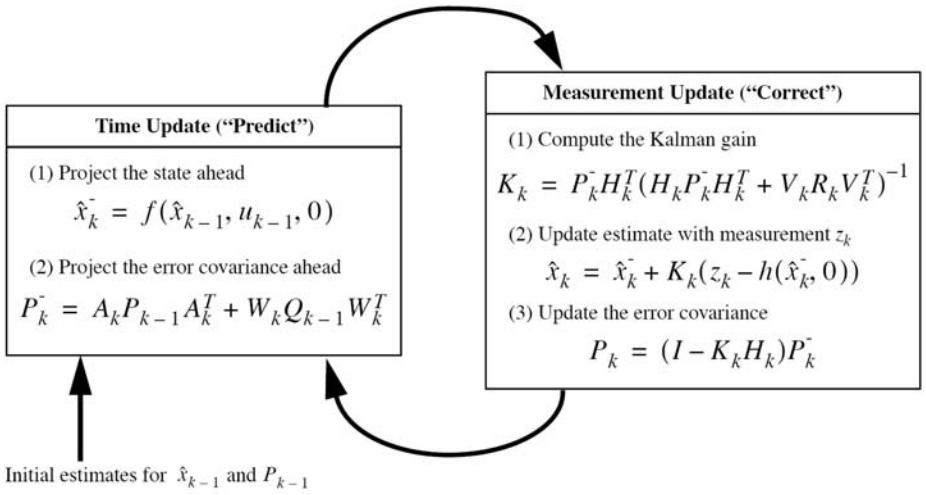

Figure 3.4: Estimation process of the extended Kalman filter, the left box is the propagation and the right box is the update process

parameters, it is said to be a negative shift in the parameter. The CuSum control chart is calculated with (3.49) and (3.50), [26].

$$S_H(i) = max[0, \bar{x}_i - (\mu_0 + K) + S_H(i-1)] \tag{3.49}$$
$$S_L(i) = max[0, (\mu_0 - K) - \bar{x}_i + S_L(i-1)] \tag{3.50}$$

Where the starting values are $S_H(0) = 0$ and $S_L(0) = 0$. $S_H(i)$ and $S_L(i)$ accumulate deviations from the target value that is greater than the reference value K, with both quantities reset to zero upon becoming negative. Care needs to be taken when choosing the value of K to minimize the chance of detecting fouling when none is, error of type 1, and not detecting fouling when fouling has occurred, error of type 2. If either $s_H(i)$ or $s_L(i)$ exceeds a constant H, the process is out of control. This constant H is the decision interval.

There are many possible ways of choosing K and it is usually chosen to be about halfway between the target mean and the mean corresponding to an out of control state.

4 Data

Since it was difficult to get access to data during this study from a cross-flow heat exchanger where fouling occurs the data used in the analysis was simulated with a Matlab program developed by Halldor Palsson and Sylvain Lalot. The program simulates time series from an unmixed cross-flow heat exchanger. A cross-flow heat exchanger test rig is now under construction at the University of Valenciennes where fouling can be induced in a controlled environment. In the following sections an introduction will be given to the model used for simulation, the fouling factor and the data used in the analysis.

4.1 Simulation model

The mathematical model of a general heat exchanger specifies the fluid temperature as position dependent fields inside the heat exchanger, where energy travel in two ways:

- By pure convection from the hot fluid to the metal sheet.
- By conduction through the metal sheet. It is assumed that the conduction within each fluid is negligible.

In the program it is possible to model the heat exchanger either with a thin metal sheet between the fluids or without the metal sheet, that is, assume that the metal sheet has negligible heat capacity. To compare the effect of the metal the output temperatures where calculated for with and without the metal sheet with the same input temperature and mass flow.

It is assumed that the cold and hot fluid flow only in x and y direction respectively. The width of the exchanger is W, the height is H and the thickness of the hot and cold passages are d_h and d_c respectively. The energy balance for this system is described by two coupled partial differential equations where the field variables are the temperatures T_c and T_h for the cold and hot side respectively. The equations are

$$\frac{\partial T_c}{\partial t} + \frac{\dot{m}_c}{\rho c H d_c}\frac{\partial}{\partial x}(cT_c) = \frac{U}{\rho c d_c}(T_h - T_c) \tag{4.1}$$

$$\frac{\partial T_h}{\partial t} + \frac{\dot{m}_h}{\rho c H d_h}\frac{\partial}{\partial y}(cT_h) = \frac{U}{\rho c d_h}(T_c - T_h) \tag{4.2}$$

In this formulation ρ and c are dependent on the flow temperature and U is dependent on both T_h and T_c as well as position x and y. Also the mass flow of the cold stream, $\dot{m}_c$, can depend on y. The mass flow of the hot stream, $\dot{m}_h$, can depend on x. Mass flow, heat transfer coefficient as well as the inflow temperatures can be time dependent.

4.2 Fouling factor

The development of fouling has been researched extensively for the last 30 years. From the beginning the industry has been pushing on further research in this field because of the financial cost of fouling in heat exchangers.

Performance of heat exchangers deteriorates with time as a result of fouling. Fouling can be accumulation of mineral deposits, rust or presence of micro-organisms on the heat transfer surfaces. These deposits increase the resistance to heat transfer and cause the rate of heat transfer to decrease. Hence the efficiency of the heat exchanger decreases. This additional resistance is represented by a fouling factor, R_f, which measures the thermal resistance introduced by fouling. For a new heat exchanger the fouling factor is zero and it increases with time as the fouling develops.

The development of fouling depends on a number of things, [2] and [6]. Major groups of fouling dependents are:

- Composition of the fluids.
- Operating conditions in the heat exchanger.
- Type and characteristics of the heat exchanger.
- Location of fouling.

- Presence of micro-organisms.

According to [2, 8] and [29] there is usually an induction time before a noticeable amount of mineral deposits has formed so the overall heat transfer coefficient changes noticeably.

Research on fouling shows that the fouling may enhance the heat transfer for a short time in the beginning of fouling due to enhanced roughness on the heat transfer surface. It has also been shown that the fouling will grow with increased rate during the fouling period, [3].

Fouling build up depends on if the flow is turbulent or not. Fouling decreases with increasing turbulence. That might explain partly why rate of fouling seems to grow as the fouling progresses since there might become situations in parts of the heat transfer surface where there is no movement of the fluids. Another possible explanation of the increasing rate of fouling might be that with the increasing roughness of the heat transfer area, the more easily the mineral deposits stick to the surface.

Resistance to heat transfer is the inverse of U. The resistance to heat transfer corresponding to fouling, R_f, is the increased resistance to heat transfer from the time that the heat exchanger is new.

$$R_f(t) = \frac{1}{U(t)A} - \frac{1}{U(0)A} \tag{4.3}$$

4.2.1 The simulated fouling

When the data was simulated the effect of fouling was introduced to the extent that the overall heat transfer coefficient, U, either decreased 20% or 50% of the value of U from a clean heat exchanger, depending on the method which was investigated. In Figure 4.1 the ratio $\frac{U_{fouled}}{U_{clean}}$ is shown. It can clearly be seen from Figure 4.1 that the effect of fouling starts slowly but increases with time as mentioned in Section 4.2.

The effect of fouling on U is calculated in the simulation with (4.4)

$$U_{\text{fouling}} = U_{\text{clean}} \cos(at + b) \tag{4.4}$$

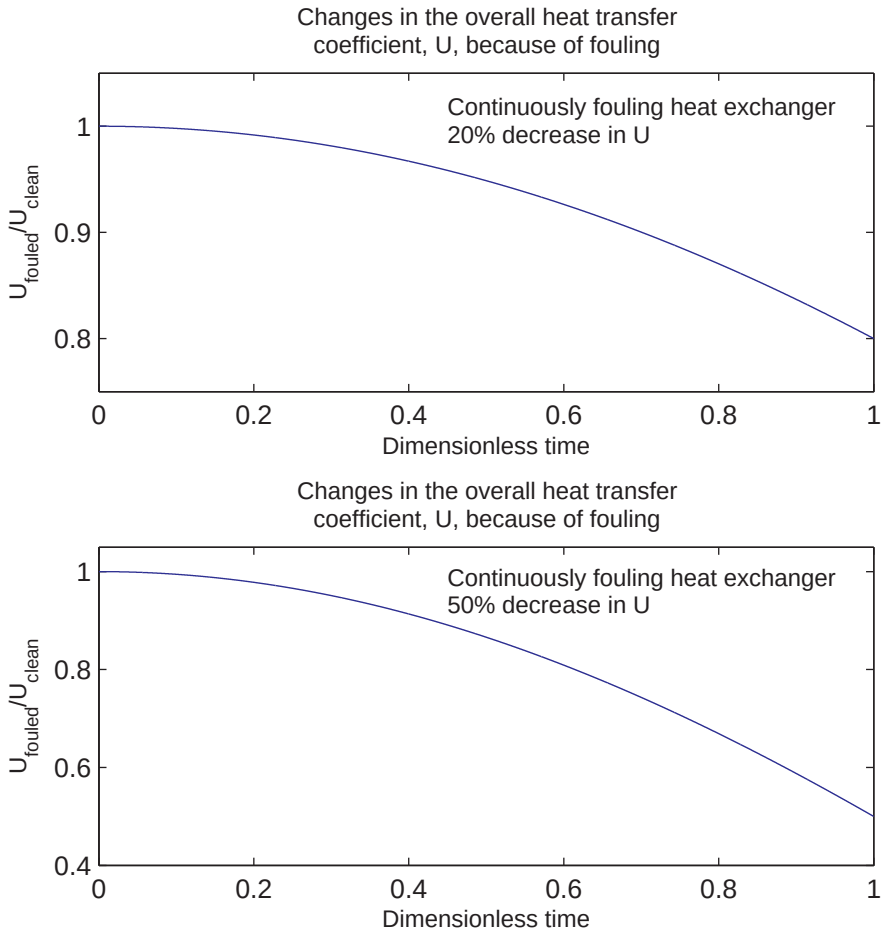

Figure 4.1: Evolution of the overall heat transfer coefficient, U, because of fouling

where

$$a = \frac{\arccos(c_{f1})}{m - \text{floor}(\text{mc}_{\text{f2}}) + 1}$$
$$b = -a(\text{floor}(\text{mc}_{\text{f2}}) + 1) \tag{4.5}$$

The constant c_{f1} indicates the value of U_{fouling} as a percent of U_{clean} from a clean heat exchanger at the end of the time series. The constant c_{f2} indicates when the fouling will start. The values of c_{f1} and c_{f2} can be between $[0, 1]$.

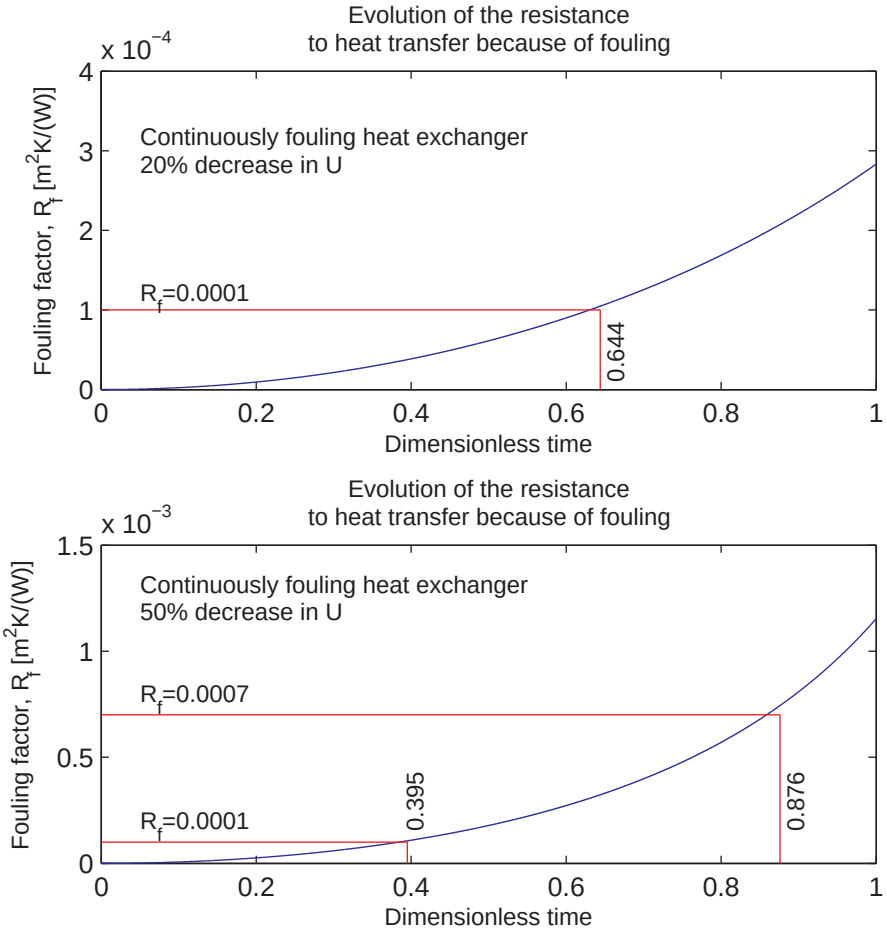

Figure 4.2: Evolution of the fouling factor R_f through the simulated time series

In Figure 4.2 the corresponding fouling factor is shown. According to [17] a fouling factor for water is typically in the range [0.0001, 0.0007]. Typical values for the fouling factor can be found at [27]. For the 20% case this interval corresponds to the [0.645, 1] in dimensionless time and for the 50% case it corresponds to the interval [0.395, 0.876] . When a heat exchanger is designed a fouling factor is chosen, the fouling factor indicates how much fouling the heat exchanger can sustain before it needs to be cleaned.

4.3 Used data

The time series from the simulation was chosen to had a resolution of 0.01 second between each simulated data point. When the time series were used in the derived methods they were down-sampled to a resolution of 1 second between each data point. The reason for simulating with more resolution was to get a more realistic simulated data.

The simulated heat exchanger was 0.5 meters wide and height and had a depth of 0.002 meters for both the hot and the cold side. The reason for these dimensions was to simulate a a turbulent flow in the heat exchanger.

The inlet temperatures and the mass flows where chosen by randomly choosing base points over certain interval. The temperatures and the mass flows where then allowed to vary between the base points by interpolating randomly between the base points.

The methods derived in Chapter 3 are for different types of heat exchanger operations. The **off-line** and **on-line methods** are designed to detect fouling in heat exchangers where the inputs vary considerable while the **slope method** is designed to detect fouling where there are small variations in the inputs. Because of the difference between the methods they need two different types of data.

In all the time series the first 25% of the time series was simulated without fouling effect, after that the fouling started.

4.3.1 Data for the off-line and on-line methods

In a pre-study of the **off-line** and **on-line method** it was apparent that a 20% decrease in U, comparing to U if no fouling was allowed, see Figure 4.1, was sufficient to detect fouling.

In all the data simulations the same fouling effect was used, in order to be able to compare the results for the methods and to do sensitivity analysis on their results. Figure 4.3 shows one of the simulated time series used in the analysis.

In the simulation the following values were used for the specific heat, $c_h = c_c = 4200$ [J/Kg°C] and the density of the fluids, $\rho = 998$ [kg/m^3]. For the **off-line** and **on-line methods** the average mass flows were 1 l/s for both the hot and cold flow. The overall heat transfer coefficient can therefore be calculated with a reference mass flow of 1 l/s to be $U = 3.780$ [W/m^{2}K] with (3.26), [6].

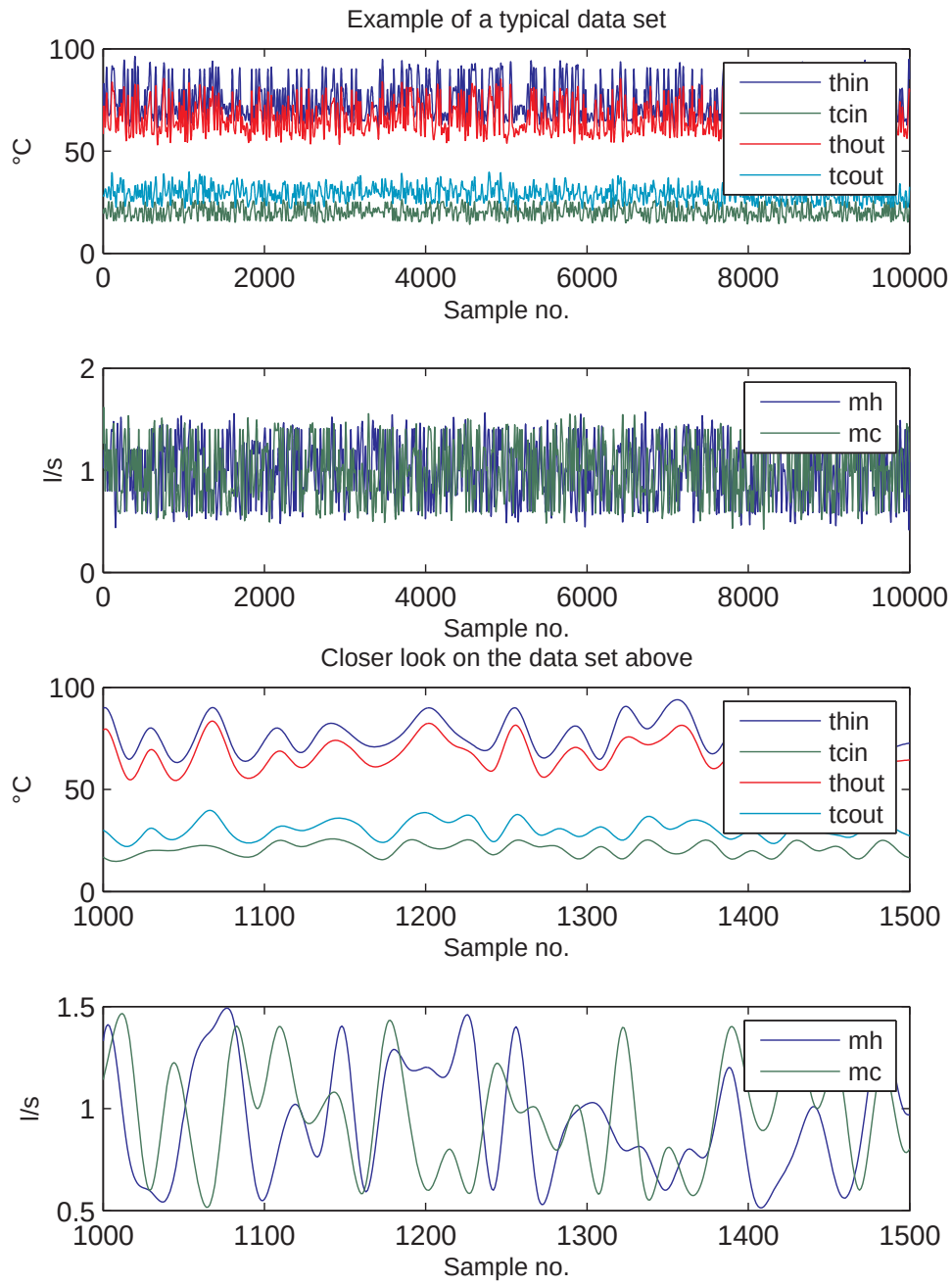

Figure 4.3: Simulated data

Since the specific heat, density of the fluids and the overall heat transfer coefficient is given it is possible to calculate the expected values of the parameters in the model. As is mentioned in Section 3.2 the model has 4 sections on the hot side and 4 sections on the cold side and two mass flows on each side, see Figure 3.1. The expected values of the parameters can therefore be calculated by using the following equations:

$$\alpha = \frac{A_{h,ij}U}{\dot{m}_h c_h} = \frac{(WH/4)U}{(\dot{m}_h/2)c_h}$$
$$\beta = \frac{A_{c,ij}U}{\dot{m}_c c_c} = \frac{(WH/4)U}{(\dot{m}_c/2)c_c}$$
$$\tau_h = \frac{M_{h,ij}}{\dot{m}_h} = \frac{WHd\rho/4}{(\dot{m}_h/2)}$$
$$\tau_c = \frac{M_{c,ij}}{\dot{m}_c} = \frac{WHd\rho/4}{(\dot{m}_c/2)}$$

Table 4.1 shows the expected values of the parameters.

Table 4.1: Calculated values of the parameters in the model

Calculated values of the parameters	
θ	$E[\theta]$
α	0.1125
β	0.1125
τ_h	0.2495
τ_c	0.2495
y	0.8

4.3.2 Data for the slope method

Since the **slope method** is designed to detect fouling in heat exchangers with small variations in their inputs it was not possible to use the same data as used in the **off-line** and **on-line methods**. The fouling was allowed to decrease U to 50% of U from a clean heat exchanger, see Figure 4.1, and the variations in the data are much less and closer to steady state. Figure 4.4 shows one of the used data sets.

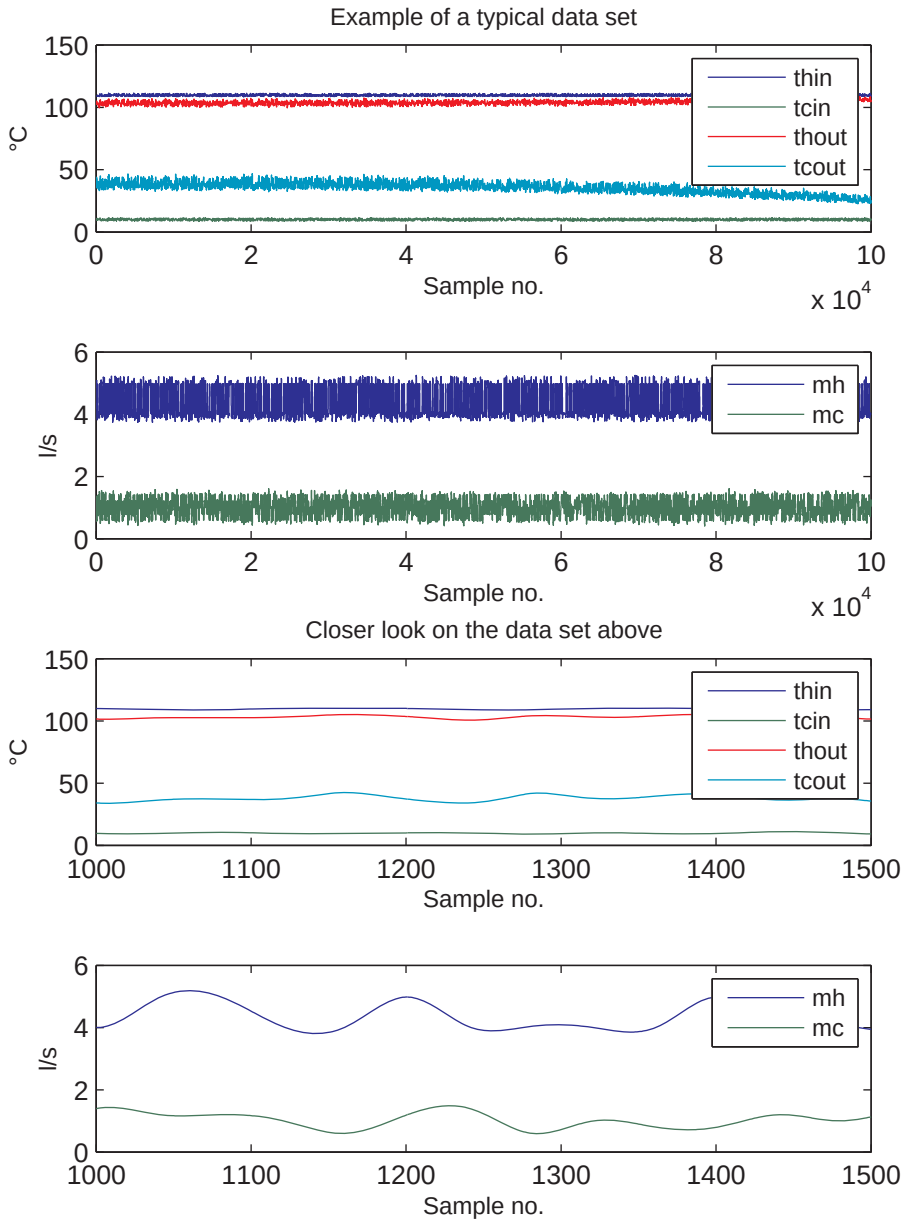

Figure 4.4: Data set used in the **slope method**

5 Results

In this chapter the main results for the derived methods will be given. The chapter starts with the **off-line method** where the standard Kalman filter is used to estimate the states of the model. Then the on-line method is described where the extended Kalman filter was used to estimate the states of the model. In the end the results of the **slope method** are given.

Simulating data with the metal sheet needs considerable more computing time than simulating data without the metal sheet, because of the difference in simulation time a comparison was done on these two different data simulations. During the comparison two data sets were simulated that had exactly the same inputs T_{hin}, T_{cin}, $\dot{m}_h$ and $\dot{m}_c$. The outputs T_{hout} and T_{cout} were then calculated either with or without the metal sheet. After the analysis of the effect of the metal, a sensitivity analysis on the detection of fouling was done.

The following assumptions, unless otherwise stated, were used in the study:

- All the sections on the hot side have the same α.
- All the sections on the cold side have the same β.
- The hot and the cold side have equal heat exchange area.

5.1 Off-line method

The minimizing algorithm used to minimize the score function was the function `fmincon` in Matlab.

In this section the following will be studied:

- Parameter estimation.
- Sensitivity for initial values.
- Sensitivity for the sampling time.
- Increased number of α and β parameters.

In the end of this section the results for the method will be given along with a sensitivity analysis of the detection.

5.1.1 Parameter estimation

The unmeasurable states in the model are estimated by the Kalman filter, see Section 3.4, and the parameters are estimated by minimizing the mean-square estimation error.

In addition to estimating the parameters the minimum routine, `fmincon`, also estimates the Hessian matrix, also known as the Fisher´s information matrix, [9]. By using the diagonal of the inverse of the estimated Hessian matrix from the minimum routine and the value of the score function with the estimated parameters it is possible to get the variance of the estimated parameters by using (5.1). By using the variance of the estimation the 95% interval can be calculated for the parameters.

$$\mathbf{Cov}[(\underline{\hat{\theta}})] = \frac{2\mathbf{V}((\underline{\hat{\theta}}))}{N-(t_1+p)}H^{(-1)} \tag{5.1}$$

where p is the number of estimated parameters.

To compare the difference between the data when the metal is included and when not included in the simulation, the same part of the two data series were used to estimate the parameters of the model. Table 5.1 shows the estimated values of the parameters

when the metal was included in the simulation. Table 5.2 shows the estimated values of the parameters when the metal was not included in the simulation. From the tables it is apparent that there is a difference in the estimation of the parameters if the metal is included or not in the simulation. It can also be seen in Tables 5.1 and 5.2 that the 95% interval for the τ values include zero which indicates that the method has difficulty when estimating them. Further analysis of the difference will be done in the following sections.

Table 5.1: Estimation of the parameters and corresponding 95% interval when the effect of the metal is included

Estimated parameters, with the metal				
	θ	$\sigma(\theta)$	**2.5%**	**97.5%**
α	0.0944	0.0004	0.0937	0.0951
β	0.1037	0.0004	0.1029	0.1045
τ_h	0.006	0.29	-0.56	0.57
τ_c	0.01	1.08	-2.1	2.1
y	0.81	0.014	0.78	0.84

Table 5.2: Estimation of the parameters and corresponding 95% interval when the effect of the metal is neglected

Estimated parameters, without the metal				
	θ	$\sigma(\theta)$	**2.5%**	**97.5%**
α	0.110	0.0003	0.1094	0.1106
β	0.114	0.0003	0.1129	0.1142
τ_h	0.02	0.15	-0.3	0.3
τ_c	0.04	0.85	-1.6	1.7
y	0.81	0.01	0.79	0.83

Figure 5.1 shows how well the model predicts the output temperatures. It can be seen that the predictions are following the actual process very well, which indicates that the model is a good representation of the process.

In order to analyze the performance better an analysis of the residuals was performed. Figures 5.2 and 5.3 show the residuals and the autocorrelation of the residuals respectively. Figure 5.3 shows that there is some correlation in the residuals, this can be expected when the data in Figure 4.3 is analyzed, in the figure it can be seen that due to slow variations the observation $x(t + \Delta)$, where Δ is few time steps, is highly correlated to observation $x(t)$.

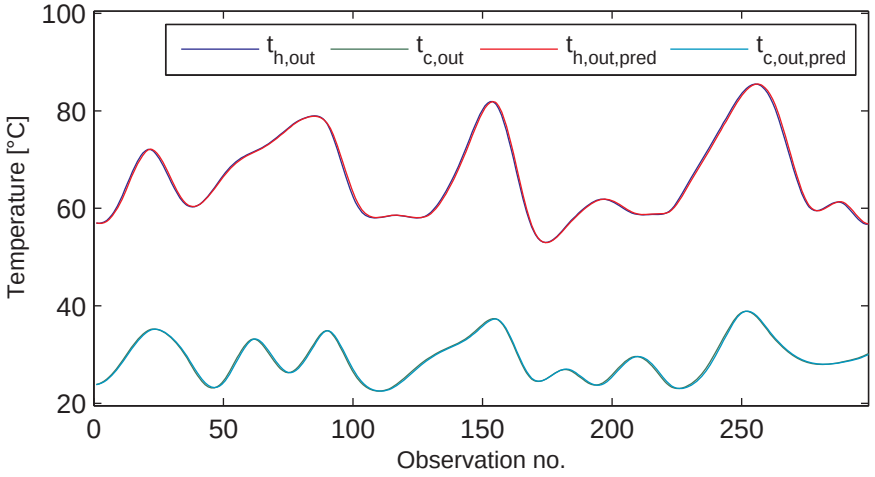

Figure 5.1: Prediction of the process

5.1.2 Effect of initial values

In order to test if the method is sensitive to initial values, one hundred random initial values on the interval [0, 2] were tried.

The result was that in all cases the Kalman filter managed to estimate the states of the model. The minimizing algorithm gave the values of α, β and y close to their calculated values, see Table 4.1. The method had difficulties estimating τ_h and τ_c. The estimated values for τ_h and τ_c were from the lower limit, 0.001, to 0.05. Statistical analysis of the sensitivity of initial values are given in Table 5.3.

It can be seen in Table 5.3 that there is a difference in the estimated values for α and β at sixth decimal, which indicates that the estimation process is quite consistent.

It can be concluded that the method is indifferent to the initial values of the parameters.

5.1.3 Different sampling steps

In effort to minimize computing time, analysis of sensitivity of the model to different sampling steps was tried. Table 5.4 shows that the sampling step does not have a considerable effect on the estimation of the α, β and y, as before the method has

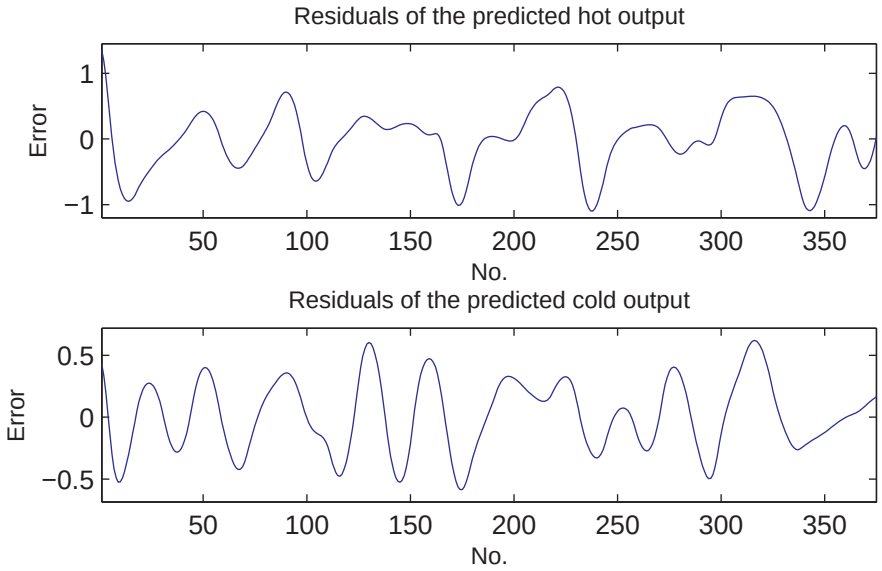

Figure 5.2: Residuals between the predicted and observed

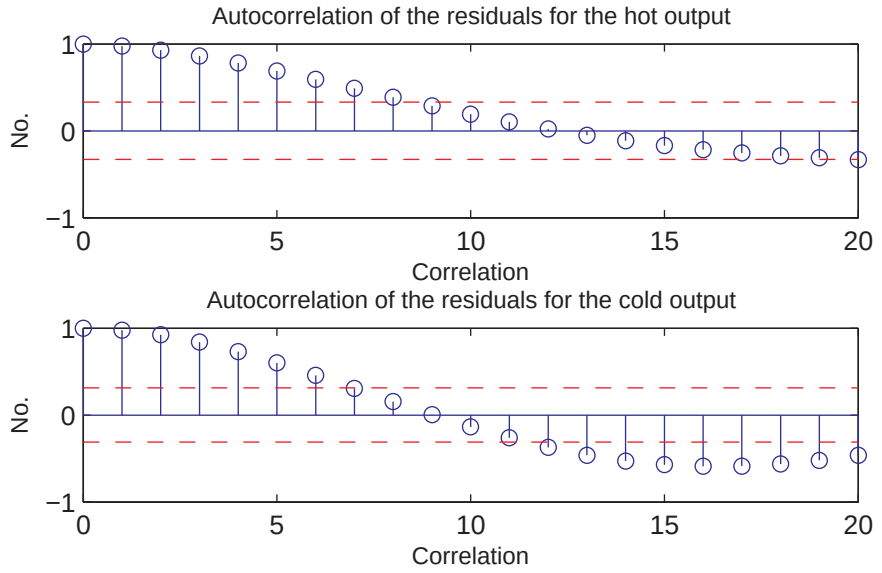

Figure 5.3: Autocorrelation of the residuals

Table 5.3: Statistical results of the estimated values from 100 different initial values

Statistical results from sensitivity analysis of 100 initial values			
θ	$E[\theta]$	$\sigma[\theta]$	[2.5%, 97.5%] percentiles
α	0.0889627	0.0005	[0.0889622, 0.0889639]
β	0.0958743	0.0005	[0.0958738, 0.0958753]
τ_h	0.0140	0.008	[0.001, 0 .0229]
τ_c	0.0175	0.01	[0.001, 0.0284]
y	0.8228	0.01	[0.8228, 0.8228]

difficulties when estimating τ_h and τ_c.

Table 5.4: Estimation of the parameters with different sampling time

Sampling time	α	β	τ_h	τ_c	**y**
1	0.0950	0.1041	0.0010	0.0325	0.8071
2	0.0949	0.1041	0.0494	0.0627	0.8041
3	0.0951	0.1041	0.0363	0.0244	0.8069
4	0.0948	0.1041	0.0572	0.0193	0.7962
5	0.0947	0.1042	0.0268	0.0277	0.7995
6	0.0946	0.1044	0.0251	0.0294	0.8043
7	0.0951	0.1040	0.0248	0.0215	0.7997
8	0.0950	0.1042	0.0234	0.0336	0.8029
9	0.0956	0.1042	0.0998	0.2317	0.8221
10	0.0957	0.1040	0.3361	0.4336	0.8206

5.1.4 Increased number of α and β parameters

Since the fouling detection is done through α and β it would be beneficial to estimate more α and β parameters and use those α and β parameters to detect where the fouling is occurring in the heat exchanger. In (3.16) the different α and β parameters are denoted with the subscript ij, which indicates which section in the model they belong to.

In Section 5.1 it is shown that the method has difficulties estimating the τ values, they where therefore kept fixed in this study with their calculated values, see section 4.3. To decrease the number of parameters needed to be estimated y was also kept fixed to 0.8, as is recommended in [6].

In this study $\alpha_1 = \alpha_{11} = \alpha_{21}$, $\alpha_2 = \alpha_{12} = \alpha_{22}$, $\beta_1 = \beta_{11} = \beta_{12}$ and $\beta_2 = \beta_{21} = \beta_{22}$. Where the indicator ij corresponds to the indicators in Figure 3.1.

The method did not manage to estimate the α and β parameters. Although it was interesting that the average value of the α and β parameters was close to the expected values of the parameters. The conclusion is that the method has difficulties when estimating more than one α and β parameters.

5.1.5 Detection of fouling using the off-line method

When the **off-line method** is used to detect fouling, the parameters of the model are estimated over a fixed and moving window of specific size. In this study the window size was chosen to be 200 observations. Longer window would give less variation of the estimated parameters between the windows, but the downside is that a longer window requires more calculations and hence more computer time. In this case the window was moved 20 observations ahead between estimations. The step between the windows should be chosen in accordance with the expected fouling, if a fast fouling is expected than it might be reasonable to have short intervals between adjacent windows. If on the other hand a slow fouling is expected it might be feasible to save computing time by having longer interval between adjacent windows.

To save computational time only the first window got random initial values for the parameters. All the following estimations had the initial values of the parameters equal to the estimated parameters in the previous window. This is considered reasonable since the parameters are not expected to change abruptly between adjoining windows and it has been shown that the method is invariant to the initial values of the parameters.

As is mentioned in Section 3.2 the fouling is detected by monitoring for shifts in α and β.

When monitoring for a shift in the parameters the CuSum test was used, see Section 3.5. The expected values and standard deviation for the parameters were estimated with a part of the clean part of the parameter estimates. The reference value, K, in 3.50 and 3.49 was chosen to be the standard deviation. The CuSum chart was used to monitor the mean of the last 30 values for a shift. As before the two simulated data sets were compared.

Detection on fouling on the metal data set

Figure 5.4 shows how the parameters vary over the whole data set. It can be seen that their values are decreasing, as expected, since the heat exchanger starts accumulating

fouling at 25% in the data set. It can be seen in Figure 5.5 that drift in α is detected in 0.77 and in β in 0.40 in dimensionless time.

Detection on fouling on the data set without the metal

If Figures 5.6 and 5.7 are compared to Figures 5.4 and 5.5 respectively it can be seen that there is not much difference between the estimations and fouling detection whether the metal sheet is included or not in the simulation.

Since there is not much difference between the detection times when the effect of the metal is included and when it is not, it can be concluded that the effect of metal in the simulation can be neglected when the **off-line method** is used to detect fouling.

5.1.6 Sensitivity analysis on detection

In Section 3.2 it is mentioned that the mass flow has a considerable effect on the parameters. This effect can influence the detection of fouling. This influence was studied by simulating 20 different time series and by going through the process of detection of fouling using the **off-line method**. Of the 20 data sets the CuSum chart only had problem with 1 of the data sets. The problem was that the CuSum chart detected a shift in a parameter but the process got back to a normal state shortly after. A correct detection was made later in the data sets.

The result of this analysis was that the fouling is detected with 95% certainty between 0.35 and 0.84 in dimensionless time for the fouling factor used. This interval corresponds to a fouling factor in the interval [0.00003, 0.00018], see Figure 4.2.

5.1.7 Conclusion for the off-line method

- It can be concluded that the **off-line method** can be used to detect fouling in cross-flow heat exchangers by using measurements that are easily measured in normal operation. For the fouling used the **off-line method** detects the fouling in the interval [0.35, 0.84] in dimensionless time. The detection interval corresponds to a fouling factor on the interval [0.00003, 0.00018]. If the detection interval is compared to the fouling factors in Section 4.2 it can be seen that the method is working well. As is mentioned there, typical values for the fouling factor are in the range [0.0001, 0.0007].
- The **off-line method** had difficulties estimating the τ values in the model.
- If the results are compared to the results in Appendix A, where a slow drift was

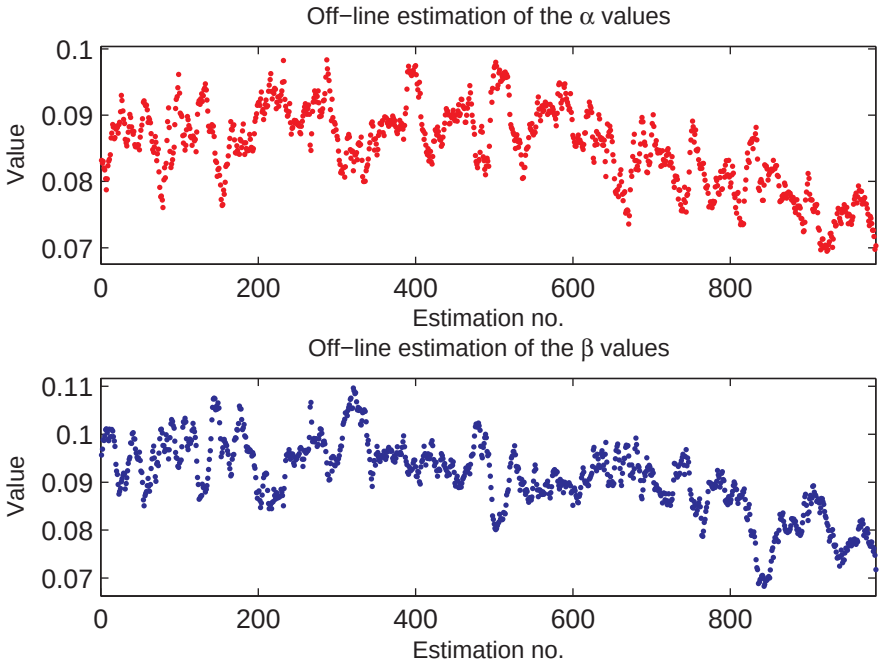

Figure 5.4: Evolution of the parameters through the sampling time, including the metal

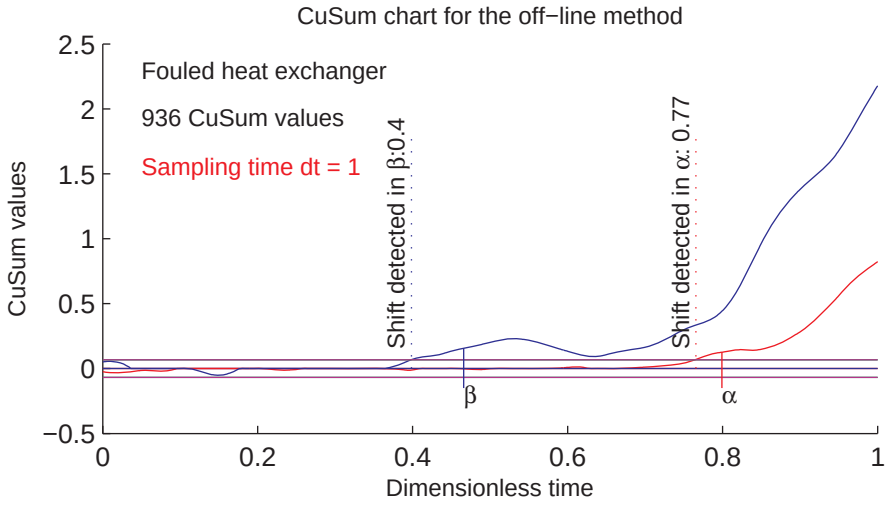

Figure 5.5: Detecting shift in the off-line estimated parameters, including the metal

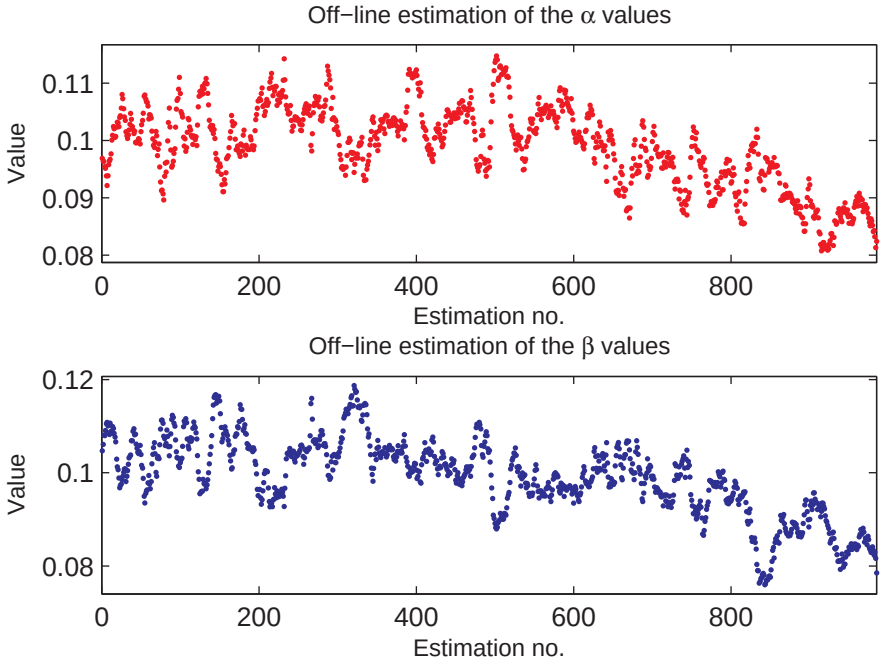

Figure 5.6: Evolution of the parameters through the sampling time, neglecting the metal

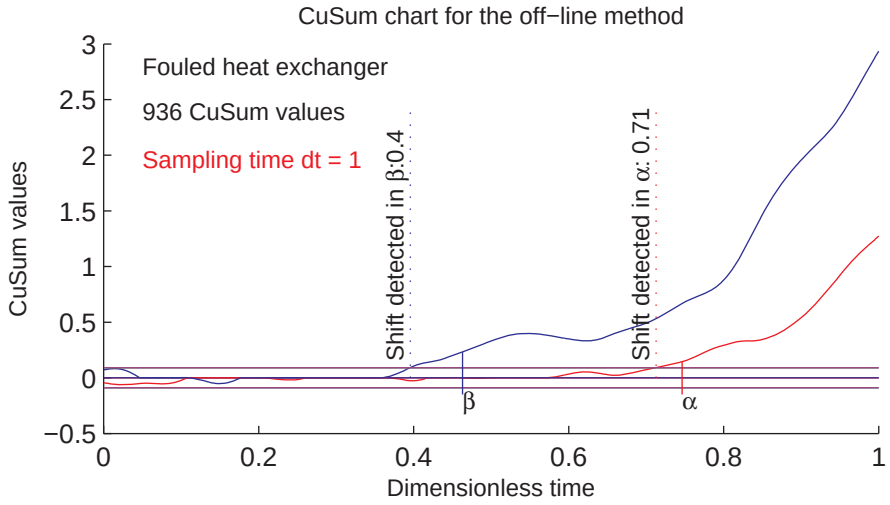

Figure 5.7: Detecting shift in the off-line estimated parameters, neglecting the metal

analyzed, it seems that the method is relatively invariant of the drift speed. It should be pointed out that only one slow drift was simulated and therefore a further investigation is needed on that subject.

5.2 On-line method

In this section α and β are formulated as states in the model and the Extended Kalman filter (EKF) is used to follow the changes in the parameters α and β as the process evolves. As mentioned in Section 3.2 the fouling is detected by monitoring for shifts in α and β. To detect the shift in the parameters the CuSum chart is used, see Section 3.5.

In this section the following will be studied:

- Step size for the parameters.
- Sensitivity for the sampling time.
- Sensitivity for initial values.
- Sensitivity for sampling time.
- Increased number of α and β parameters.

In the end of this section the results for the method will be given along with a sensitivity analysis of the detection.

5.2.1 Step size

When using the EKF to follow the parameters the parameters are allowed to move with a certain maximum step each time, the step size is controlled through the process noise defined in the covariance matrix, Q. Before further analysis is done the maximum step has to be chosen carefully so that the model will show a clear indication of changes in the parameters. If the step is to small the method will be too slow to follow changes in the parameters. On the other hand if the step is too big it will be harder to notice a clear indication of a shift in the parameters. In Figure 5.8 the different values of the constant c in the matrix, Q, is shown. In this model Q is a 10x10 matrix and $Q(1,1) = Q(2,2) = cq$ are the process noises for the parameters α and β. If the value c is chosen to be $c = 10^{-9}$ the parameter values are allowed to change 2-3% in a few sample steps. In further investigation the $c = 10^{-9}$ is used for both the data set with or without the metal sheet.

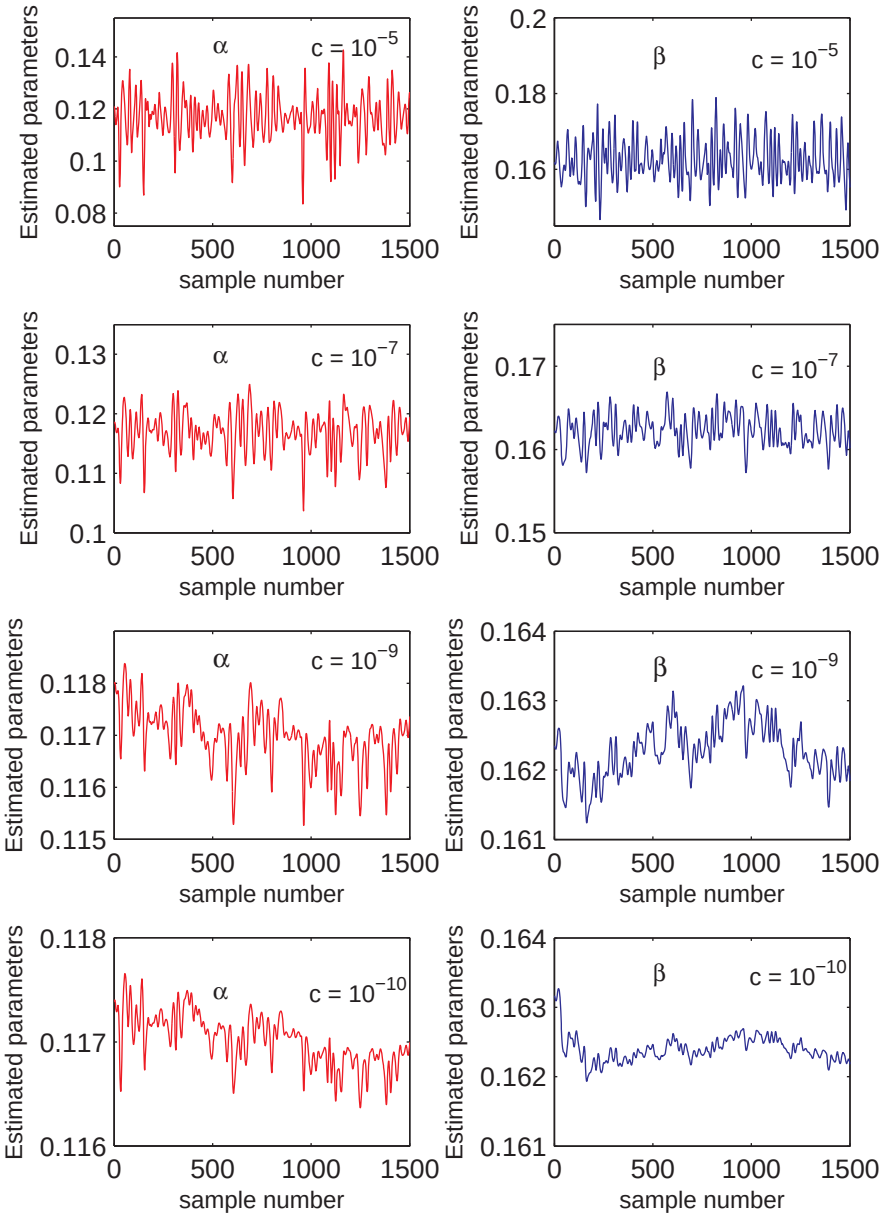

Figure 5.8: The effect of different scale of the covariance matrix Q

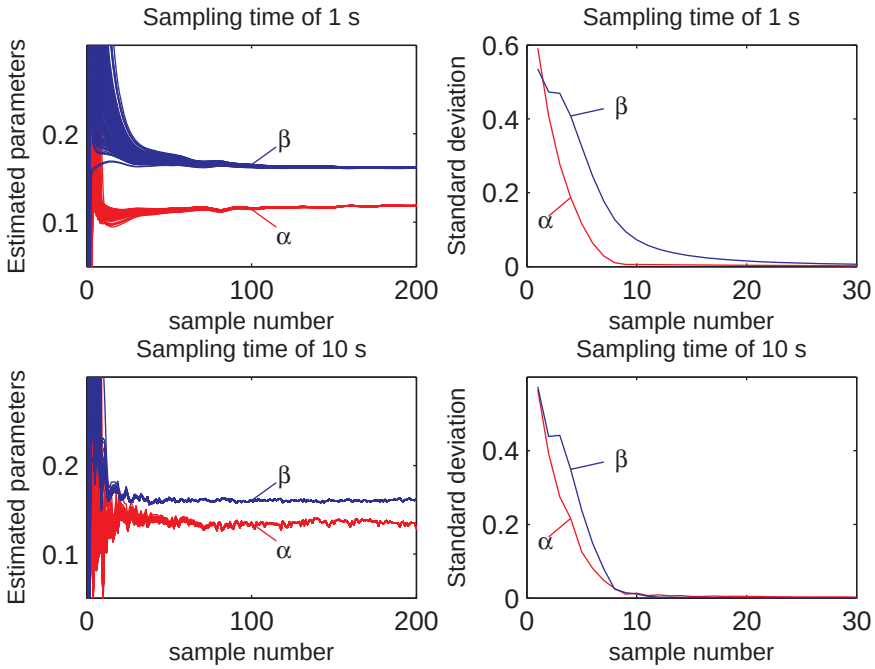

Figure 5.9: Values of α and β for a sampling time of 1 s and 10 s and evolution of the standard deviation

5.2.2 Effect of initial values and sampling time

As with the **off-line method** the effect of different initial values and sampling time was investigated.

To be sure that the effect of initial values does not play any role in the parameter estimation 100 random initial values on the interval 0 to 2 were tried out for both the α and β values. In Figure 5.9 it can be seen that the model converges relatively quickly to certain values for the parameters. The right figure shows the evolution of the standard deviation over all the 100 estimates at a given sample.

In Figure 5.10 the evolution of the standard deviation is investigated further. It can be seen that if the sampling time is 1s the standard deviation is less then 1% of the parameter value after 100 samples. For the 10s sampling time the standard deviation is less then 1% of the parameter value after 70 samples.

From Figures 5.9 and 5.10 it can be seen that the method converges relatively quick

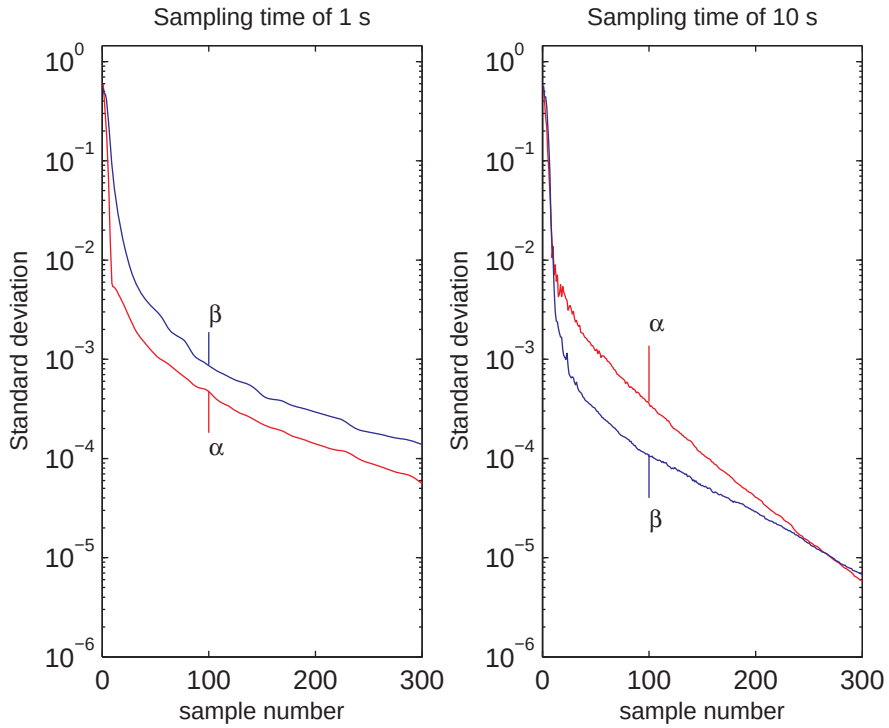

Figure 5.10: The evolution of the standard deviation of α and β for a sampling time of 1 s and 10 s in logarithm scale

even though a high sampling step is used. A sampling time as high as 200s was tried and the method converged relatively quickly, it can therefore be assumed that the method is invariant to the sampling step.

In further analysis the first 100 values will be considered as burn in for the model and is therefore not used in further analysis.

5.2.3 Detection of fouling using the on-line method

As with the off-line method the data sets with and without the metal sheet will be compared. In detection of fouling using the **on-line method** the moving average of the last 30 values of the α and β are monitored for a shift with the CuSum chart, see Section 3.5.

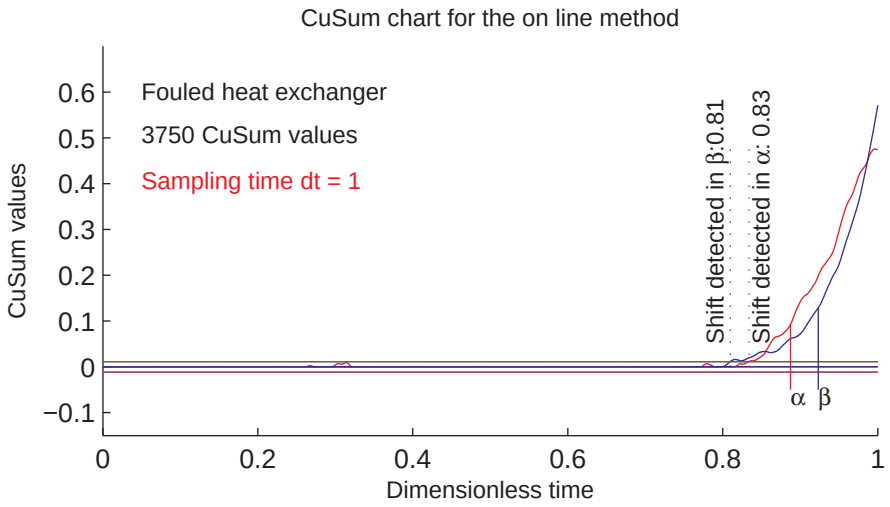

Figure 5.11: Detecting shift in the parameters with the **on-line method**, including the metal

Detection on fouling on the metal data set

In Figure 5.11 it can be seen that a shift in the β parameter is detected in 0.81 in dimensionless time and in 0.83 for the α parameter. In this analysis the sampling time is $1s$.

Detection on fouling on the data set without the metal

If Figures 5.12 and 5.11 are compared it can clearly be seen that shift in the parameters are detected at the same time. It has now been shown that the effect of the metal sheet in the data simulation can be neglected when detecting fouling using the **on-line method**.

5.2.4 Effect of increased sampling time on detection of fouling

To save computing time the effect of increased sampling time was investigated.

Figures 5.13 and 5.14 show the effect on detection of fouling when using different sampling times when estimating the parameters with the **on-line method**. It can be seen that the sampling time does not play significant role when detecting fouling. It can also be seen that the fouling is not necessarily detected in both the parameters

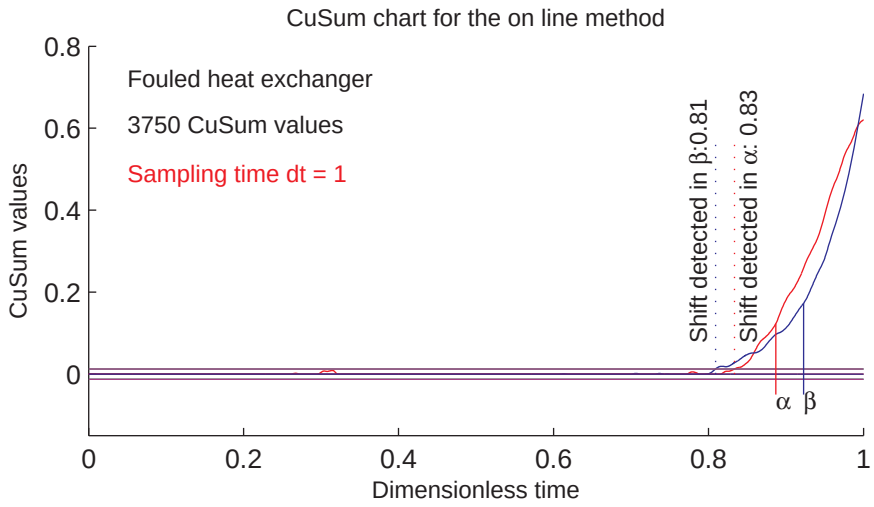

Figure 5.12: Detecting shift in the parameters with the **on-line method**, neglecting the metal

when the sampling time is increased. Is should be pointed out that when the sampling time is increased, the number of times the parameters are estimated, decreases. In the case where the sampling time was 10s there were only 375 CuSum values calculated comparing to 3.750 CuSum values when the sampling time was 1s. This difference in number of CuSum values can have some influences on the detection time.

Nevertheless it is interesting to note that even though the sampling time is increases dramatically there is still a possibility to detect fouling.

5.2.5 Sensitivity analysis on detection

A sensitivity analysis on the fouling detection was done for the **on-line method** by simulating 50 different data sets and go through the detection process with them.

The result of this analysis where that the fouling is detected with 95% certainty between 0.65 and 0.91 in dimensionless time for the fouling factor used. This interval corresponds to a fouling factor on the interval [0.0001, 0.00022], see Figure 4.2.

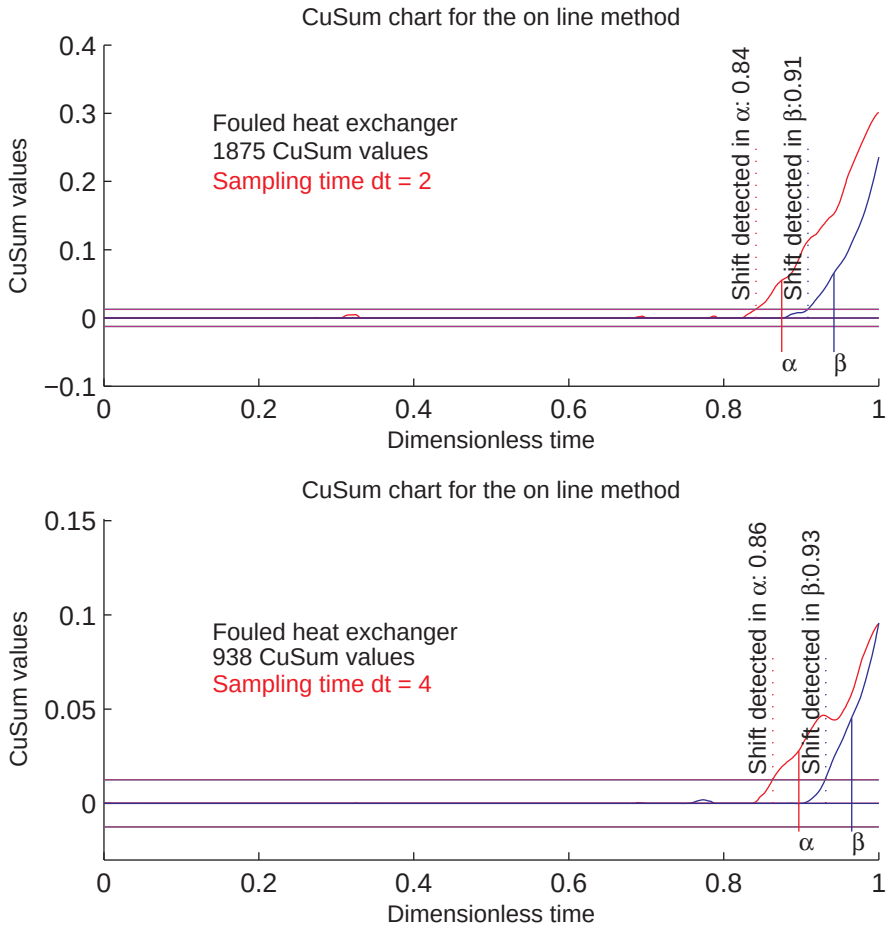

Figure 5.13: Detecting shift in the parameters with sampling times $dt = 2$ and $dt = 4$

5.2.6 Increased number of α and β parameters

As with the **off-line method** the **on-line method** was also tried with more α and β parameters. The same parameters where used as in the **off-line method**, that is $\alpha_1 = \alpha_{11} = \alpha_{21}$, $\alpha_2 = \alpha_{12} = \alpha_{22}$, $\beta_1 = \beta_{11} = \beta_{12}$ and $\beta_2 = \beta_{21} = \beta_{22}$. The indicator ij corresponds to the sections in Figure 3.1.

The method had difficulties estimating more α and β parameters. During the estimation process the parameters became unstable. The conclusion is that the method has the same difficulties when estimating more than one α and β parameters as the

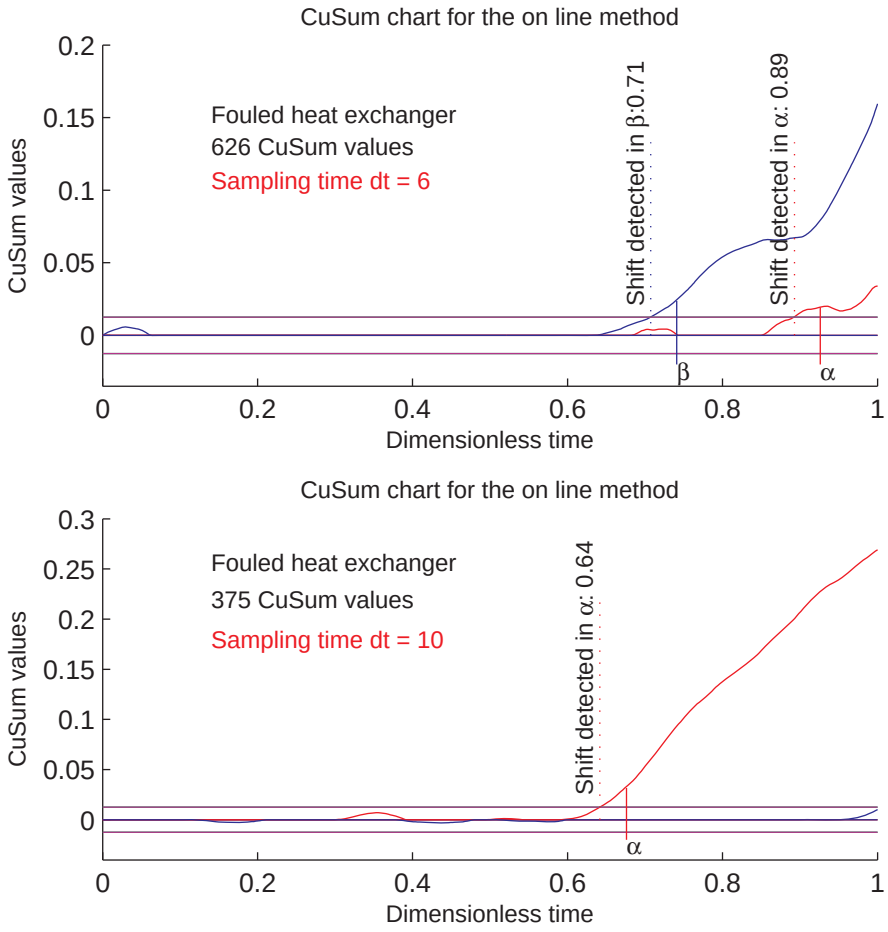

Figure 5.14: Detecting shift in the parameters with sampling times $dt = 6$ and $dt = 10$

off-line method.

5.2.7 Conclusion for the on-line method

- From the analysis of the **on-line method** it can be seen that the method can be used to detect fouling in cross-flow heat exchanger. The effect of the metal sheet can be neglected during the data simulation. For the fouling used the **on-line method** detected fouling on the interval [0.65, 0.91] in dimensionless time. The detection interval corresponds to a fouling factor in the interval [0.0001,

0.00021]. Comparison of the detection interval to typical fouling factor values, [0.0001, 0.0007], indicate that the method is giving good results.

- If the results are compared to the results in Appendix A, where a slow drift was analyzed, it seems that the method detects a slow drift sooner than a fast drift. Further investigation is however needed on that subject.
- The method has difficulties when estimating more then one α and β values.

5.3 The slope method

The **slope method**, described in Section 3.3, was derived to detect fouling in heat exchangers which usually have small variation in their inlets, as is the case for district heating heat exchangers. In district heating systems all the inlets have small variations except the cold mass flow. The cold mass flow varies with water demand. To simulate a case similar to a district heating system, data which had small variations in inlet temperatures, the hot mass flow and the cold mass flow, was allowed to vary considerably more. Due to the small variation in the data the other methods, **off-line** and **on-line method**s, were not able to estimate the parameters, and could therefore not be used to detect the fouling.

As mentioned in Section 4.3 the first 25% of the data set is from a clean heat exchanger, and in the second part of the data set the heat exchanger is gradually getting fouled. For this method the overall heat transfer coefficient, U, was allowed to decrease to 50% of the value of U for a clean heat exchanger, see Figure 4.1. In Figure 5.15 typical estimation of the reference slope is shown, the reference slope is estimated by using the clean part of the data.

In Figure 5.16 the changes in the slope, AUF, is monitored. The straight black line is the reference slope and the green line shows how the slope is changing in time. The above figure shows all the data points from all the windows the slope AUF is estimated from, in the lower figure the data points have been removed and the value of the x-axis have been changed to a dimensionless time to show how the slope is changing in time. If the slope is decreasing it can mean that the heat exchanger is accumulating fouling or that the inputs have changed.

To check statistically where the shift in the slope begins the CuSum chart was used, see Section 3.5. That is if there is a shift in $\Delta UAF = UAF_{\text{reference}} - UAF_{\text{fouling}}$. Figure 5.17 shows only the CuSum values for the fouled part of the data. The CuSum charts detects shifts in the slope at 0.42 in dimensionless time.

If the detection is compared to the fouling factors in Section 4.2 it can be seen that

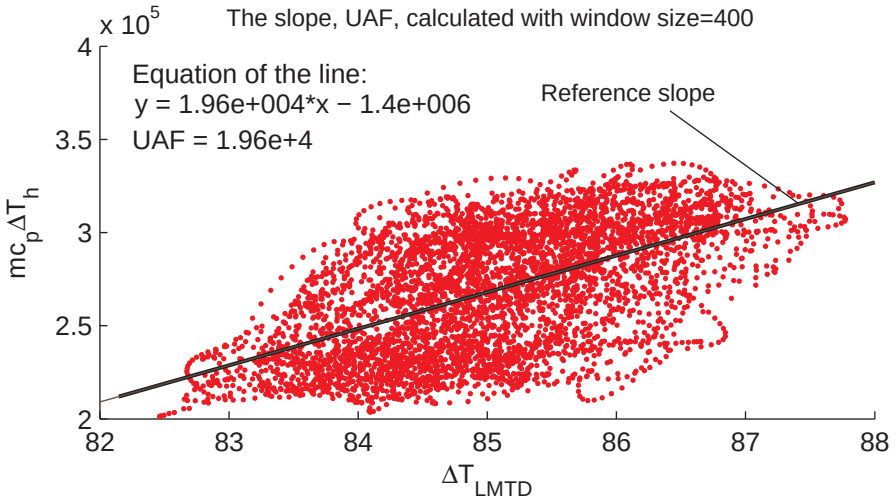

Figure 5.15: Estimation of a reference slope.

the detection corresponds to $R_f = 0.00016$ which can be considered a good result if compared to typical fouling factor values, which are in the range [0.0001, 0.0007].

5.3.1 Sensitivity analysis on detection

In Section 3.2 it is mentioned that the mass flow has considerable effect on the parameters. This effect can influence the detection of fouling. The influence was studied by simulating 50 different time series and by going through the process of detection of fouling with the **slope method**. Of the 50 data sets the **slope method** gave unstable results for 4 data sets. Those data sets were therefore excluded from the sensitivity analysis.

The result of this analysis was that the fouling is detected with 95% certainty between 0.33 and 0.92 in dimensionless time for the fouling factor used. This interval corresponds to a fouling factor on the interval [0.00007, 0.0008], see Figure 4.2.

It should be mentioned that in some cases the reference slope was either over- or underestimated, which resulted in the slope either overshooting, or undershooting the clean slope almost from the beginning. In the case where the slope was underestimated the fouling detection was made relatively late. In the case where the slope was overestimated the fouling detection was made relatively soon. These two cases explain the wide range of the detection interval. Solution to this problem might be

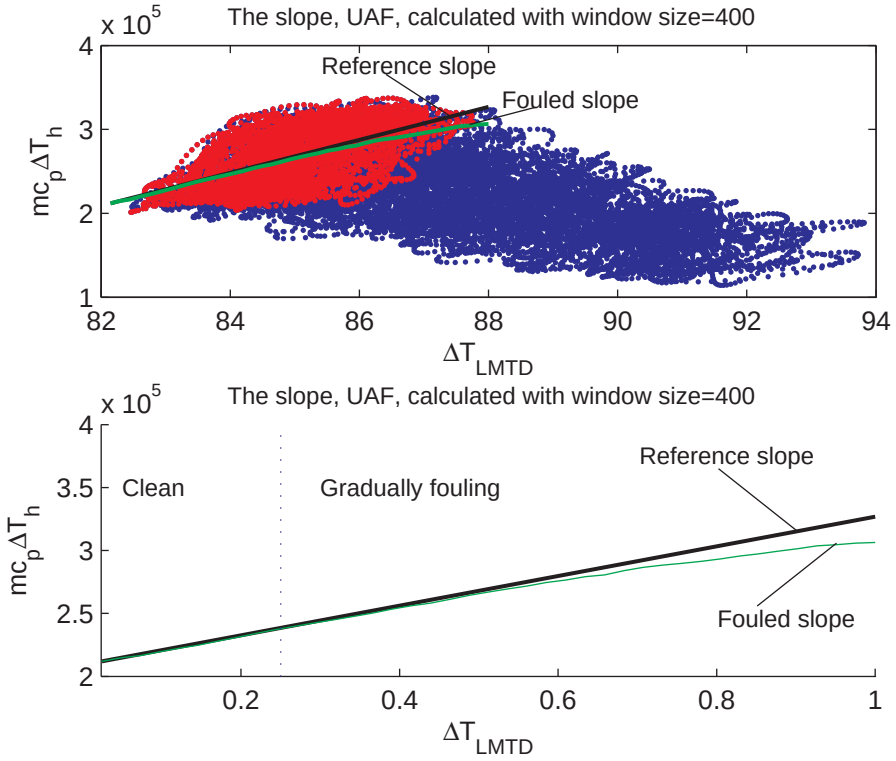

Figure 5.16: Figure a) shows all the data points from all the windows that the slope AUF is estimated from. Figure b) shows only the slopes, that is the data points have been removed, and the values of the x-axis represent a dimensionless time.

to have a longer reference interval. In this analysis the reference interval was equal to the clean part of the data.

5.3.2 Conclusion for the slope method

The **slope method** can be used to detect fouling in heat exchangers which have small variations in their inputs. The sensitivity analysis shows that the fouling detection is made when the fouling factor is in the interval [0.00007, 0.0008]. The wide range of the detection interval is due to the difficulties in estimating the reference slope. Typical fouling factor values are in the range [0.0001, 0.0007].

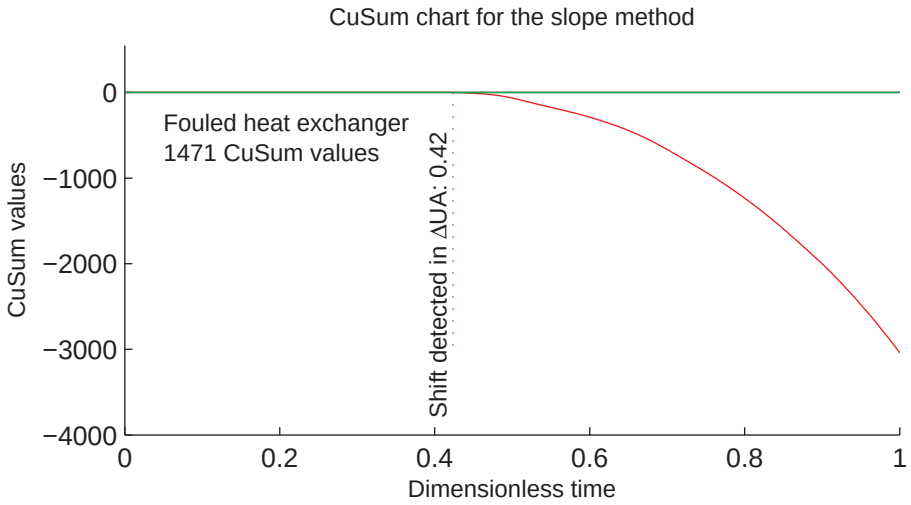

Figure 5.17: Detection of shift in the slope.

6 Discussion

The aim of the present study was to detect fouling in cross-flow heat exchangers that are either operating in a steady state condition or an unsteady condition. As mentioned in Section 2.3 heat exchangers are designed to account for the effects of fouling by incorporating a fouling factor. The fouling factor indicates the maximum fouling the heat exchanger can sustain and still fulfill it operational requirements. The fouling factor is usually on the interval [0.0001, 0.0007].

It has been shown that the methods derived can be used to detect fouling in cross-flow heat exchangers. The **off-line** and **on-line methods** are physically based models which means that some of the parameters in the model include the heat transfer coefficient of the heat exchanger. Since the parameters in the model are time varying it is possible to monitor for changes in the heat transfer coefficient due to fouling. The model parameters are estimated with either the standard or extended Kalman filter, depending on which method is used. It has been shown that the methods are not sensitive to initial values or sampling time. When fouling is introduced the parameters change drastically and that shows that the methods are well suited to detect fouling in cross-flow heat exchangers. If there are small variations in the inputs of the heat exchanger the previously mentioned methods are not suitable. In that case the **slope method** can be used to detect fouling.

In all cases the detection analysis was only used on the fouled part of the data, that is the fouling begins in 0 in dimensionless time. The main results were the following:

- **Off-line method**
  - The 95% detection interval for the off-line method is [0.35, 0.84] in dimensionless time, which corresponds to the fouling factor interval [0.00003, 0.00018].

  - The method estimates the α, β and y parameters in the model quite well but has problems with the τ_h and τ_c parameters.
  - The method cannot estimate more than one α and β.
  - The initial values of the parameters make no difference in the estimation.
  - The method can detect fouling even though the sampling time is decreased considerably.

- **On-line method**
  - The 95% detection interval for the on-line method is [0.65, 0.91] in dimensionless time, which corresponds to the fouling factor interval [0.0001, 0.00021].
  - The initial values of the parameters make no difference in the estimation.
  - The method can detect fouling even though the sampling time is decreased considerably.
  - Sufficient training period for the on-line method is the 150 first values.
  - The method cannot estimate more than one α and β.

- **Slope method**
  - The slope method can detect fouling in a heat exchanger with a small variation of the inlet variables.
  - The 95% detection interval for the slope method is [0.33, 0.92] in dimensionless time, which corresponds to the fouling factor interval [0.00007, 0.0008].

If the results of the **off-line method** are compared to the results of the **on-line method** it can be seen that the **off-line method** detects fouling faster than the **on-line method**.

It can be concluded that it is possible to detect fouling in a cross-flow heat exchanger both with small and big fluctuations in the inputs with the methods derived in this study. If there are big fluctuations, the **off-line** and **on-line methods** are used. If the fluctuations are small, the **slope method** should be used.

Since this kind of a study of cross-flow heat exchangers has not been published yet, as far as the author knows, the results are compared to similar studies done on counter-flow heat exchangers. In [16] a fouling is detected in a counter-flow tube-in-tube heat exchanger when the fouling factor was $R_f \approx 0.00008$. If those results are compared to the results for the cross-flow heat exchanger the conclusion can be drawn that the methods are working equally well.

7 Future studies

Future studies that build up from this study might be to:

- Use these methods on data from a controlled situation in a test rig cross-flow heat exchanger.
- Increase the number of sections in the model and see if it gives better results.
- Extend the physical model by incorporating more physics into the model to see if it is possible to estimate more α and β parameters. If so, then see if it is possible to detect where the fouling is forming in the heat exchanger.
- To investigate if the slope method detects fouling in counter- and parallel-flow heat exchangers and also on a data from a controlled situation in test rig cross-flow heat exchanger.

Bibliography

[1] Alfa Laval AB. http://www.alfalaval.com, product: Heat transfer.

[2] B. Bansal and X.D. Chen. Fouling of heat exchangers by dairy fluids - a review, June 2005. http://services.bepress.com/eci/heatexchanger2005/.

[3] M.W. Bohnet. Crystallization fouling on heat transfer surfaces - 25 years research in braunschweig, June 2005. http://services.bepress.com/eci/heatexchanger2005/.

[4] Robert G. Brown and Patrick Y.C. Hwang. *Introduction to Random Signals and Applied Kalman Filtering.* John Wilet and sons, 3 edition, 1997.

[5] T. Casanuevea-Robles and T.R. Bott. The environmental effect of heat exchanger fouling: a case study, June 2005. http://services.bepress.com/eci/heatexchanger2005/.

[6] Yunus A. Cengel and Robert H. Turner. *Fundamentals of Thermal-Fluid Sciences.* McGraw Hill, 2 edition, 2005.

[7] Xiao Dong Chen, Dolly X. Y. Li, Sean X. Q. Lin, and Necati Özkan. On-line fouling/cleaning detection by measuring electric resistance–equipment development and application to milk fouling detection and chemical cleaning monitoring. *Journal of Food Engineering*, 61, 2004.

[8] F. Fahiminia, A.P. Watkinson, and N. Epstein. Calcium sulfate scaling delay times under sensible heating conditions, June 2005. http://services.bepress.com/eci/heatexchanger2005/.

[9] Andrew Gelman, John B. Carlin, Hal S. Stern, and Donald B. Rubin. *Bayesian Data Analysis.* Chapman and Hall/CRC, 2 edition, 2003.

[10] M.A.S. Herónimo, L.F. Melo, A. Sousa Braga, P.J.B.F. Ferreira, and C. Martins. Monitoring the thermal efficiency of outled heat exchangers: a simplified method. *Experemental Thermal and Fluid Science*, 1997.

[11] P. Jakobsen and O.B. Stampe. Controlling the effectiveness of heat exchangers. *VVS*, 26, January 1990.

[12] Harpa Jonsdottir. *Stochatis Modelling of Hydrologic Systems*. PhD thesis, Technical university of Denmark - Informatics and Mathematical Modelling, 2006.

[13] G. Jonsson and O.P. Palsson. An application of extended kalman filtering to heat exchanger models. *Journal of Dynamic Systems, Measurement and Control*, 116, June 1994.

[14] G. Jonsson, O.P. Palsson, and K. Sejling. Modeling and parameter estimation of heat exchangers - a statistical approach. *Journal of Dynamic Systems, Measurement and Control*, 114, December 1992.

[15] Gudmundur Jonsson and Olafur P. Palsson. Use of empirical relations in the parameters of heat-exchanger models. *Ind. Eng. Chem. Res*, 1991.

[16] Gudmundur R. Jonsson, Sylvain Lalot, Olafur P. Palsson, and Bernard Desmet. Use of extended kalman filtering in detecting fouling in heat exchangers. *International Journal of Heat and Mass Transfer*, 2006.

[17] S. Lalot, O.P. Palsson, G.R. Jonsson, and B. Desmet. Comparison of neural networks and kalman filters performances for fouling detection in a heat exchanger. *International Journal of Heat Exchangers*, VII, 2007.

[18] S. Lecoeuche, S. Lalot, and B. Desmet. Modelling a non-stationary single tube heat exchanger using multiple coupled local neural networks. *International Communications in Heat and Mass Transfer*, 32, 2005.

[19] Larry J. Levy. The kf: Navigation's integration workhorse. http://www.cs.unc.edu/ welch/kalman/Levy1997/Levy1997KF_Workhorse.pdf.

[20] Bay Industrial Instruments Limited. Fouling in heat exchangers - quarterly newsletter. http://www.bayindustrial.com/FoulingInHeatExchangers.pdf.

[21] Henrik Madsen. *Time series analysis*. IMM - DTU, 2 edition, 2006.

[22] Douglas C. Montgomery and George C. Runger. *Applied Statistics and Probability for Engineers*. John Wiley and Sons, Inc., 3 edition, 2002.

[23] Arthur G.O. Muambara and Marwan S.Y. Al-Haik. Ekf based parameter estimation for a heat exchanger, , 1999.

[24] A. Nejim, C. Jeynes, Q. Zhao, and H. Müller-Steinhagen. Ion implantation of stainless steel heater alloys for anti-fouling applications, 1999.

[25] P.K. Nema and A.K. Datta. A computer based solution to check the drop in milk outlet temperature due to fouling in a tubular heat exchanger. *Journal of Food Engineering*, 2005.

[26] 2008 NIST/SEMATECH e-Handbook of Statistical Methods. http://www.itl.nist.gov/div898/handbook/.

[27] Engineering Page. http://www.engineeringpage.com/engineering/thermal.html.

[28] S.S. Ramachandra, S. Wiehe, M.M. Hyland, X.D. Chen, and B. Bansal. A preliminary study of the effect of surface coating on the initial deposition mechanisms of dairy fouling, June 2005. http://services.bepress.com/eci/heatexchanger2005/.

[29] G. Rizzo, H. Müller-Steinhagen, and E. Richter. Induction period if heterogeneous nucleation during crystallisation fouling: Ion implantation effects, June 2005. http://services.bepress.com/eci/heatexchanger2005/.

[30] Sepehr Sanaye and Behzad Niroomand. Simulation of heat exchanger network (hen) and planning the optimum cleaning schedule. *Energy Conversion and Management*, February 2007.

[31] Reinate Steinhagen, Hans Müller-Steinhagen, and Kambiz Maani. Problems and fosts due to heat exchanger fouling in new zealand industries. *Heat transfer engineering*, 14, January 1993.

[32] Greg Welch and Gary Bishop. An introduction to the kalman filter, , updated July 24, 2006.

[33] Wikipedia. http://en.wikipedia.org/.

[34] Peter M. Withers. Ultrasonic, acoustic and optical techniques for the non-invasive detection of fouling in food processing equipment. *Elsevier Science Ltd.*, 1996.

A Long drift

In Chapter 5 a fast drift was studied. To see if the drift speed of the fouling matters, the fouling time was doubled and the same analysis done on that data.

In the following sections a brief introduction of the data set is given and the main results are given for all the methods.

A.1 Data

The same fouling factor was used as for the data sets used in Chapter 5, see Section 4.2. In Chapter 5 it is concluded that there is not much difference whether the metal is simulated or not. Therefore the metal is not simulated in this analysis.

Figure A.1 shows the simulated time series.

A.2 Off-line method

It is assumed that the analysis done on the off-line method in Chapter 5 is valid here. Therefore only the detection part was done. The main difference between the analysis done here and in Section 5.1 is that here the window was moved 40 observations ahead in stead of just 20 observations in the analysis of the slow drift. The reason was to decrease the computer time.

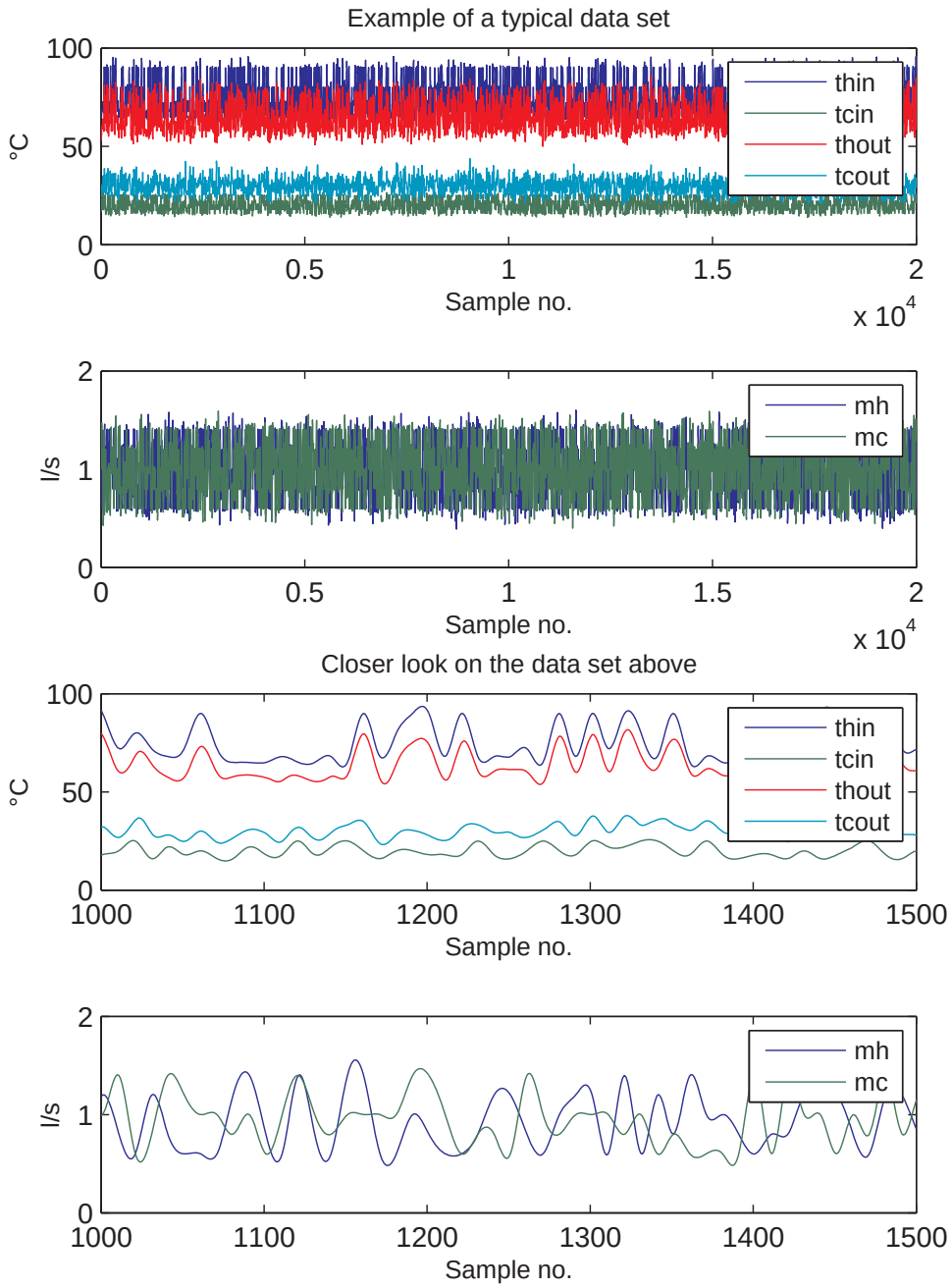

Figure A.1: Simulated data

Table A.1: Estimation of the parameters and corresponding 95% interval when the effect of the metal is neglected

Estimated parameters, without the metal					
	θ	$Var(\theta)$	**2.5%**	**97.5%**	
α	0.1095	0.0003	0.0733	0.1458	Significant
β	0.1167	0.0004	0.0769	0.1565	Significant
τ_h	0.0293	0.7794	-1.7364	1.7950	Not significant
τ_c	0.0227	1.2530	-2.2161	2.2615	Not significant
y	0.8084	0.0132	0.5788	1.0380	Significant

A.2.1 Parameter estimation

Table A.1 shows the estimated values of the parameters in the model.

When comparing the values to Table 5.2 it can be seen that the estimated values are very similar.

In further analysis the τ values were kept fixed since they are not correctly estimated by the model.

A.2.2 Detection of fouling using the off-line method

Figure A.2 shows how the parameters varied over the whole data set. It can clearly be seen that their values are decreasing, as expected since the heat exchanger starts accumulating fouling 25% in the data set.

As mentioned in Section 3.2 the fouling is detected by monitoring for shifts in α and β.

In Figure A.3 a drift in α is detected in 0.44 and in β in 0.34 in dimensionless time.

A.3 On-line method

It is assumed that the analysis done on the on-line method in Chapter 5 is valid here. Therefore only the detection part was done.

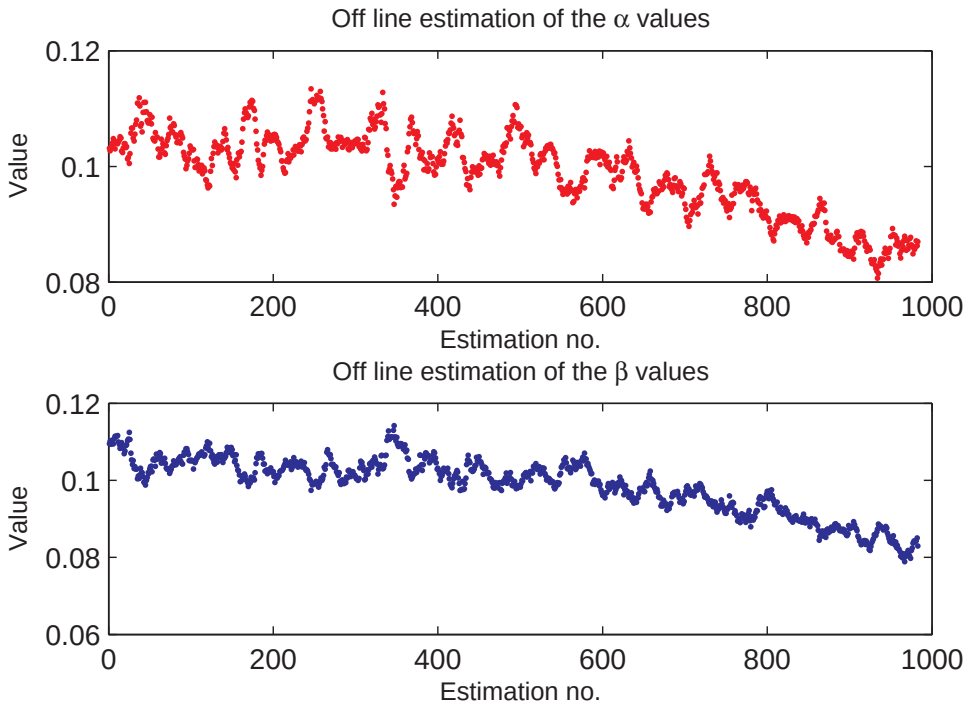

Figure A.2: Evolution of the parameters through the sampling time

A.3.1 Detection of fouling using the on-line method

In Figure A.4 it can be seen that a shift in the β parameter is detected in 0.66 in dimensionless time and in 0.76 for the α parameter.

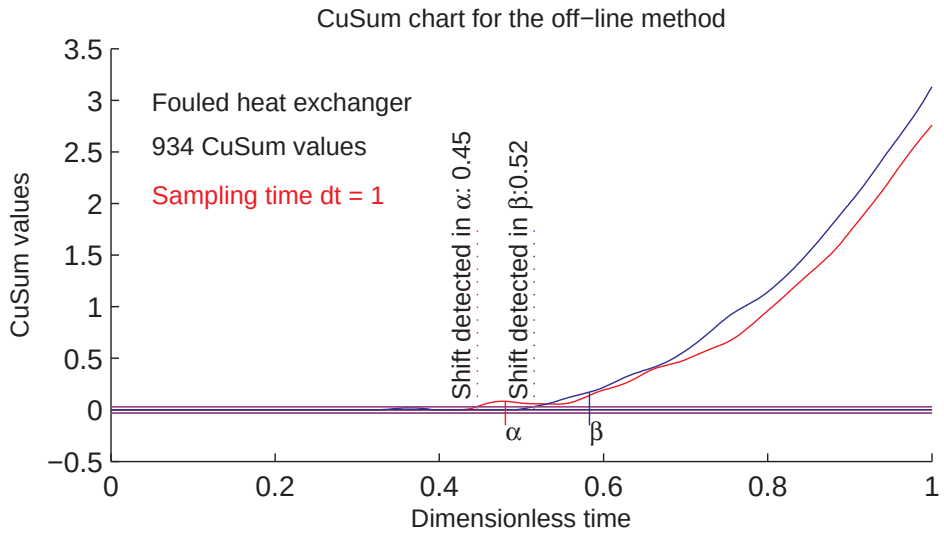

Figure A.3: Detecting shift in the off-line estimated parameters

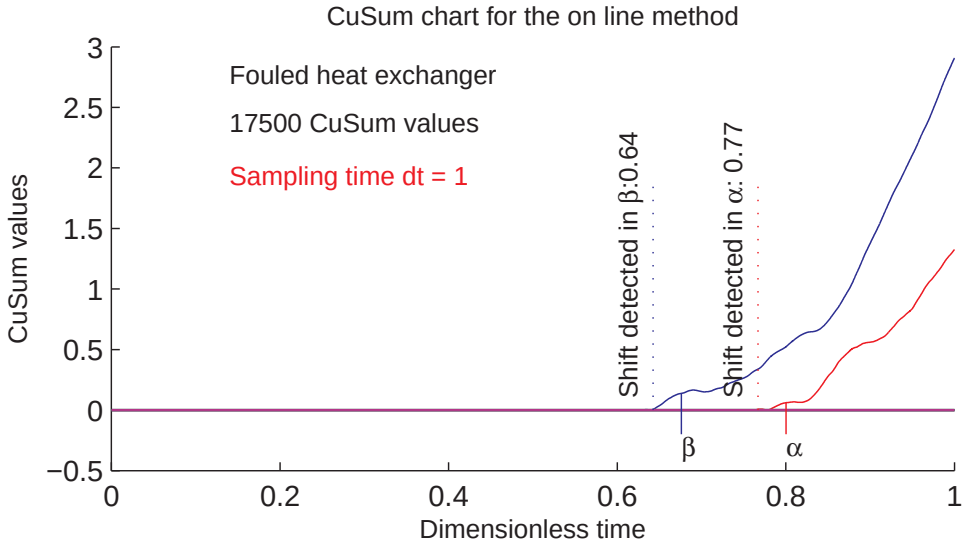

Figure A.4: Detecting shift in the parameters with the on-line method

B The calculations of F

To get F it is necessary to calculate the 80 derivatives in (3.37). By quick inspection of (3.36) it can be seen that most of the derivatives will become zero.

Following are the derivatives of f_1:

$$\frac{\partial f_1}{\partial \alpha} = \frac{1}{2\tau_h}(-T_{h,10} - T_{h,11} + T_{c,01} + T_{c,11})$$

$$\frac{\partial f_1}{\partial T_{h,11}} = -\frac{1+\alpha/2}{\tau_h}$$

$$\frac{\partial f_1}{\partial T_{c,11}} = \frac{\alpha}{2\tau_h}$$

$$\frac{\partial f_1}{\partial \beta} = \frac{\partial f_1}{\partial T_{h,12}} = \frac{\partial f_1}{\partial T_{h,21}} = \frac{\partial f_1}{\partial T_{h,22}} = \frac{\partial f_1}{\partial T_{c,12}} = \frac{\partial f_1}{\partial T_{c,21}} = \frac{\partial f_1}{\partial T_{c,22}} = 0$$

Following are the derivatives of f_2:

$$\frac{\partial f_2}{\partial \alpha} = \frac{1}{2\tau_h}(-T_{h,11} - T_{h,12} + T_{c,02} + T_{c,12})$$

$$\frac{\partial f_2}{\partial T_{h,11}} = \frac{1-\alpha/2}{\tau_h}$$

$$\frac{\partial f_2}{\partial T_{h,12}} = -\frac{1+\alpha/2}{\tau_h}$$

$$\frac{\partial f_2}{\partial T_{c,12}} = \frac{\alpha}{2\tau_h}$$

$$\frac{\partial f_2}{\partial \beta} = \frac{\partial f_2}{\partial T_{h,21}} = \frac{\partial f_2}{\partial T_{h,22}} = \frac{\partial f_2}{\partial T_{c,11}} = \frac{\partial f_2}{\partial T_{c,21}} = \frac{\partial f_2}{\partial T_{c,22}} = 0$$

Following are the derivatives of f_3:

$$\frac{\partial f_3}{\partial \alpha} = \frac{1}{2\tau_h}(-T_{h,20} - T_{h,21} + T_{c,11} + T_{c,21})$$
$$\frac{\partial f_3}{\partial T_{h,21}} = -\frac{1+\alpha/2}{\tau_h}$$
$$\frac{\partial f_3}{\partial T_{c,11}} = \frac{\alpha}{2\tau_h}$$
$$\frac{\partial f_3}{\partial T_{c,21}} = \frac{\alpha}{2\tau_h}$$
$$\frac{\partial f_3}{\partial \beta} = \frac{\partial f_3}{\partial T_{h,11}} = \frac{\partial f_3}{\partial T_{h,12}} = \frac{\partial f_3}{\partial T_{h,22}} = \frac{\partial f_3}{\partial T_{c,12}} = \frac{\partial f_3}{\partial T_{c,22}} = 0$$

Following are the derivatives of f_4:

$$\frac{\partial f_4}{\partial \alpha} = \frac{1}{2\tau_h}(-T_{h,21} - T_{h,22} + T_{c,12} + T_{c,22})$$
$$\frac{\partial f_4}{\partial T_{h,21}} = \frac{1-\alpha/2}{\tau_h}$$
$$\frac{\partial f_4}{\partial T_{h,22}} = -\frac{1+\alpha/2}{\tau_h}$$
$$\frac{\partial f_4}{\partial T_{c,12}} = \frac{\alpha}{2\tau_h}$$
$$\frac{\partial f_4}{\partial T_{c,22}} = \frac{\alpha}{2\tau_h}$$
$$\frac{\partial f_4}{\partial \beta} = \frac{\partial f_4}{\partial T_{h,11}} = \frac{\partial f_4}{\partial T_{h,12}} = \frac{\partial f_4}{\partial T_{c,11}} = \frac{\partial f_4}{\partial T_{c,21}} = 0$$

Following are the derivatives of f_5:

$$\frac{\partial f_5}{\partial \beta} = \frac{1}{2\tau_c}(T_{h,10} + T_{h,11} - T_{c,01} - T_{c,11})$$
$$\frac{\partial f_5}{\partial T_{h,11}} = \frac{\beta}{2\tau_c}$$
$$\frac{\partial f_5}{\partial T_{c,11}} = -\frac{1+\beta/2}{\tau_c}$$
$$\frac{\partial f_5}{\partial \alpha} = \frac{\partial f_5}{\partial T_{h,12}} = \frac{\partial f_5}{\partial T_{h,21}} = \frac{\partial f_5}{\partial T_{h,22}} = \frac{\partial f_5}{\partial T_{c,12}} = \frac{\partial f_5}{\partial T_{c,21}} = \frac{\partial f_5}{\partial T_{c,22}} = 0$$

Following are the derivatives of f_6:

$$\frac{\partial f_6}{\partial \beta} = \frac{1}{2\tau_c}(T_{h,11} + T_{h,12} - T_{c,02} - T_{c,12})$$

$$\frac{\partial f_6}{\partial T_{h,11}} = \frac{\beta}{2\tau_c}$$

$$\frac{\partial f_6}{\partial T_{h,12}} = \frac{\beta}{2\tau_c}$$

$$\frac{\partial f_6}{\partial T_{c,12}} = -\frac{1+\beta/2}{\tau_c}$$

$$\frac{\partial f_6}{\partial \alpha} = \frac{\partial f_6}{\partial T_{h,21}} = \frac{\partial f_6}{\partial T_{h,22}} = \frac{\partial f_6}{\partial T_{c,11}} = \frac{\partial f_6}{\partial T_{c,21}} = \frac{\partial f_6}{\partial T_{c,22}} = 0$$

Following are the derivatives of f_7:

$$\frac{\partial f_7}{\partial \beta} = \frac{1}{2\tau_c}(T_{h,20} + T_{h,21} - T_{c,11} - T_{c,21})$$

$$\frac{\partial f_7}{\partial T_{h,21}} = \frac{\beta}{2\tau_c}$$

$$\frac{\partial f_7}{\partial T_{c,11}} = \frac{1-\beta/2}{\tau_c}$$

$$\frac{\partial f_7}{\partial T_{c,21}} = -\frac{1+\beta/2}{\tau_c}$$

$$\frac{\partial f_7}{\partial \alpha} = \frac{\partial f_7}{\partial T_{h,11}} = \frac{\partial f_7}{\partial T_{h,12}} = \frac{\partial f_7}{\partial T_{h,22}} = \frac{\partial f_7}{\partial T_{c,12}} = \frac{\partial f_7}{\partial T_{c,22}} = 0$$

Following are the derivatives of f_8:

$$\frac{\partial f_8}{\partial \beta} = \frac{1}{2\tau_c}(T_{h,21} + T_{h,22} - T_{c,12} - T_{c,22})$$

$$\frac{\partial f_8}{\partial T_{h,21}} = \frac{\beta}{2\tau_c}$$

$$\frac{\partial f_8}{\partial T_{h,22}} = \frac{\beta}{2\tau_c}$$

$$\frac{\partial f_8}{\partial T_{c,12}} = \frac{1-\beta/2}{\tau_c}$$

$$\frac{\partial f_8}{\partial T_{c,22}} = -\frac{1+\beta/2}{\tau_c}$$

$$\frac{\partial f_2}{\partial \alpha} = \frac{\partial f_2}{\partial T_{h,11}} = \frac{\partial f_2}{\partial T_{h,12}} = \frac{\partial f_2}{\partial T_{c,11}} = \frac{\partial f_2}{\partial T_{c,21}} = 0$$

List of Figures

List of Tables